PERGAMON

Journal of Structural Geology 21 (1999) 511–532

JOURNAL OF STRUCTURAL GEOLOGY

Neotectonics in the eastern North Anatolian fault region (Turkey) advocates crustal extension: mapping from SAR ERS imagery and Digital Elevation Model

Jean Chorowicz[a,*], Damien Dhont[a], Niyazi Gündoğdu[b]

[a]Département de Géotectonique, ESA-CNRS 7072, case 129, Université Paris 6, 4 Place Jussieu, 75252 Paris, Cedex 05, France
[b]Department of Geology, Hacettepe University, Beytepe, Ankara, Turkey

Received 4 June 1998; accepted 6 January 1999

Abstract

This paper concerns the neotectonics of the eastern part of the Anatolian block bounded, respectively, to the north and the east by the North Anatolian (NAF) and the East Anatolian faults (EAF), meeting at Karlıova. The study is based on imagery of Synthetic Aperture Radar (SAR), scenes acquired by the European Remote Sensing (ERS) satellite and on views of a Digital Elevation Model (DEM), complemented with fault analysis in the field. We show that extensional tectonics associated with transcurrent displacements prevail in the Karlıova triangle and beyond. New local releasing bends or pull-apart basins and push-up structures along the NAF have been demonstrated. More importantly, Anatolia is composed of blocks less than 50 km in width, that are tilted and move relative to each other. They are compatible with a detachment within the crust of Anatolia. We argue that an escape wedge has migrated through time from west to east, with successive jumps to form the present-day Karlıova triangle. At each stage, the escape wedge was easterly bounded by a NE–SW-striking fault zone similar to the EAF. In each escape wedge, clockwise block rotations predate strike-slip tectonics along the N110°E-striking NAF. This is the case for instance for the Erzincan Basin where the first movements were parallel to the SW-striking Ovacık Fault, an early equivalent of the EAF, and turned later to the west. The detached crustal blocks moved southwestward, then westward and extended at the same time in order to occupy the increasing surface within the successive escape wedges. This is not the behaviour of simple lateral extrusion of the Anatolian lithospheric block induced by forces applied at its boundaries by the adjacent plates, but rather that of detached crustal blocks submitted to extension as a consequence of backward retreat of the Hellenic slab and buoyancy forces arising from crustal thickness differences.

1. Introduction

Anatolia has been defined as a lithospheric continental plate, extruded to the west in response to the N–S relative convergence of Eurasia and Africa–Arabia (McKenzie, 1972; Şengör et al., 1985; Dewey et al., 1986). This lateral tectonic escape (Burke and Şengör, 1986) occurs in between two strike-slip faults; the dextral North Anatolian (NAF) and the sinistral East Anatolian (EAF) faults, respectively, which meet at the Karlıova triangle in Eastern Anatolia, in a configuration we shall refer to as the 'escape wedge' (Fig. 1a).

In Western Anatolia, extension (McKenzie, 1978; Mercier et al., 1989) is a consequence of the opening of the Aegean back-arc basin related to northeastward subduction of the Central Mediterranean oceanic lithosphere belonging to the African plate (Le Pichon and Angelier, 1979). Extension has been described in the east as far as the Central Anatolia plateau (Pasquarè et al., 1988; Toprak and Göncüoğlu, 1993; Dhont et al., 1998b) and possibly at Karlıova (Şengör, 1979; Şengör et al., 1985; Dewey et al., 1986; Pasquarè et al., 1988; Tutkun and Hancock, 1990). Eastern Turkey,

* Corresponding author.
E-mail address: choro@lgs.jussieu.fr (J. Chorowicz)

0191-8141/99/$ - see front matter
PII: S0191-8141(99)00022-X

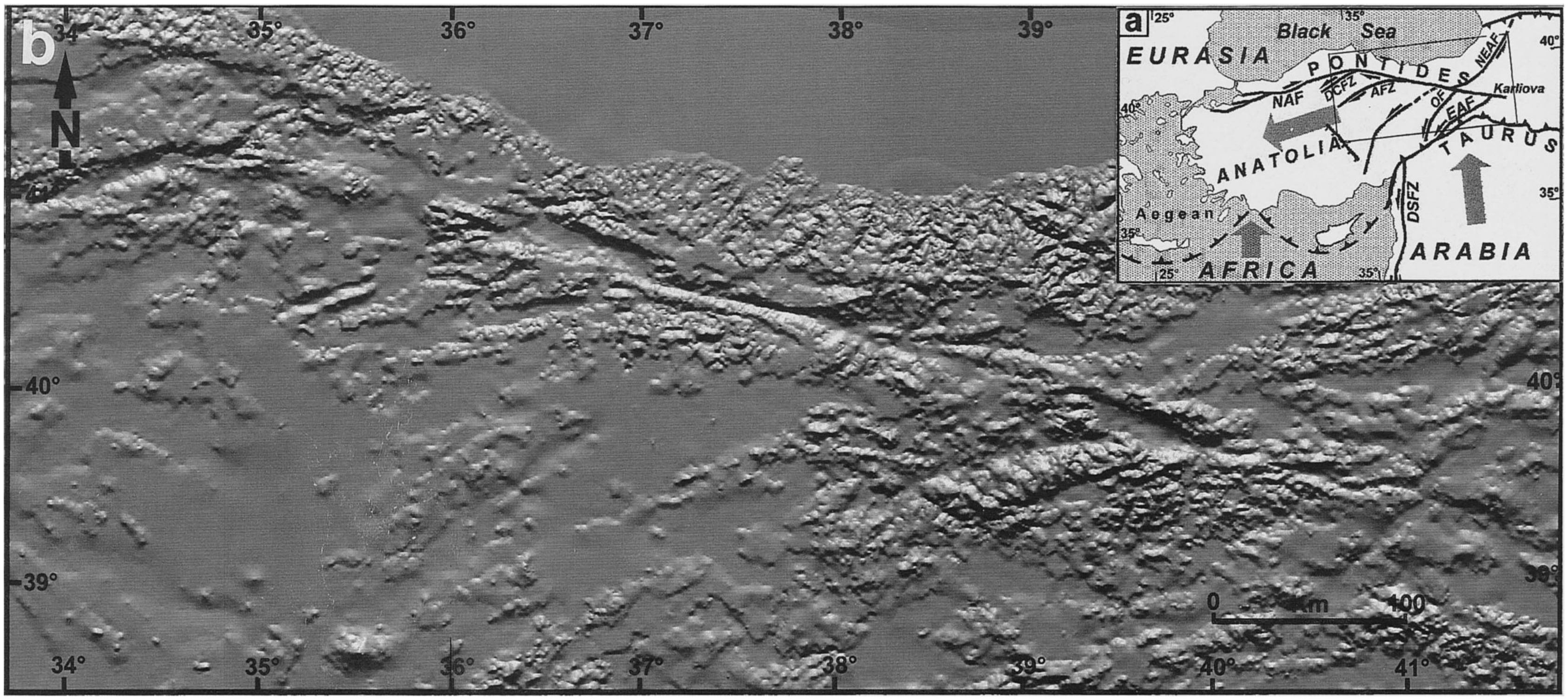

Fig. 1. (a) Tectonic context of the Anatolian region, compiled from Şengör (1979), Hancock and Barka (1981), Dewey et al. (1986), Chorowicz et al. (1994, 1995a,b). The frame is the location of the Digital Elevation Model of (b) (studied area). Large arrows represent relative plate motions within the Eurasian reference (Reilinger et al., 1997). AFZ, Almus Fault Zone; DCFZ, Devrez Çay Fault Zone; DSFZ, Dead Sea Fault Zone; EAF, East Anatolian Fault; NAF, North Anatolian Fault; NEAF, North-East Anatolian Fault; OF, Ovacık Fault. (b) Shadowed image of the Digital Elevation Model (DEM) of Central and Eastern Anatolia. This DEM is generated by linear interpolation of digitized elevation contour lines at 1/1 000 000 scale derived from the Digital Chart of the World. Ground resolution is 300 m. Illumination is from the north. (c) Fault pattern from maps, DEM and satellite image interpretations. AF, Almus Fault; d, dykes; DCFZ, Devrez Çay Fault Zone; EAF, East Anatolian Fault; Er, Erzincan; HF, Hamidiye Fault; Ha, Havza; Ka, Kazova; KB, Kargı–Bafra line; Kg, Kargı; Ko, Kolkit; La, Ladik; NAF, North Anatolian Fault; Ni, Niksar; OF, Ovacık Fault; r, Riedels; Re, Reşadiye; Ss, Suşehri; Su, Suluova; Ta, Tanyeri; Ye, Yedisu. Grey shading represents main Neogene–Quaternary basins.

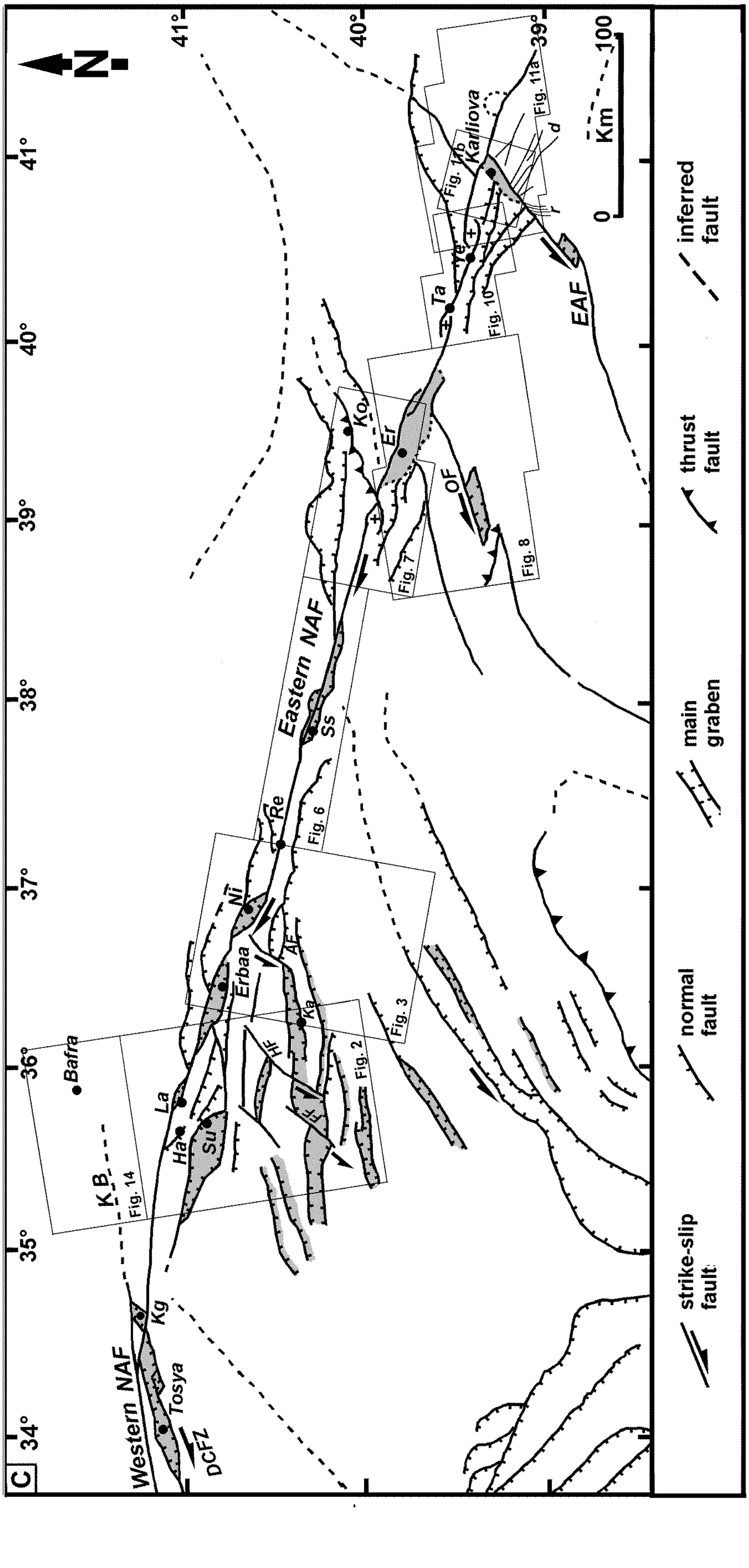
C
N
Western NAF
DCFZ
Tosya
Kg
K B
Fig. 14
Bafra
La
Ha
Su
Fig. 2
HF
Ka
Erbaa
AF
Ni
Fig. 3
Re
Fig. 6
Ss
Eastern NAF
Fig. 7
Fig. 8
OF
Er
Ko
Ta
Ye
Fig. 10
Fig. 11b
Fig. 11a
Karliova
d
r
EAF
34°
35°
36°
37°
38°
39°
40°
41°
39°
40°
41°
0
100
Km
strike-slip fault
normal fault
main graben
thrust fault
inferred fault

Fig. 1c.

Fig. 2. Interpretation of a mosaic of SAR ERS images (negative view, ascending orbit, looking ENE) of the Havza area (location in Fig. 1c). FF, strike-slip fault; LB, Ladik Basin; NAF, North Anatolian Fault. T patterns represent dip and strike of major tilted blocks.

including the Karlıova escape wedge, is supposed to be submitted to compression or strike-slip tectonics (e.g. Barka and Gülen, 1988; Yılmaz, 1993), implicating both N–S collision and west-directed lateral extrusion

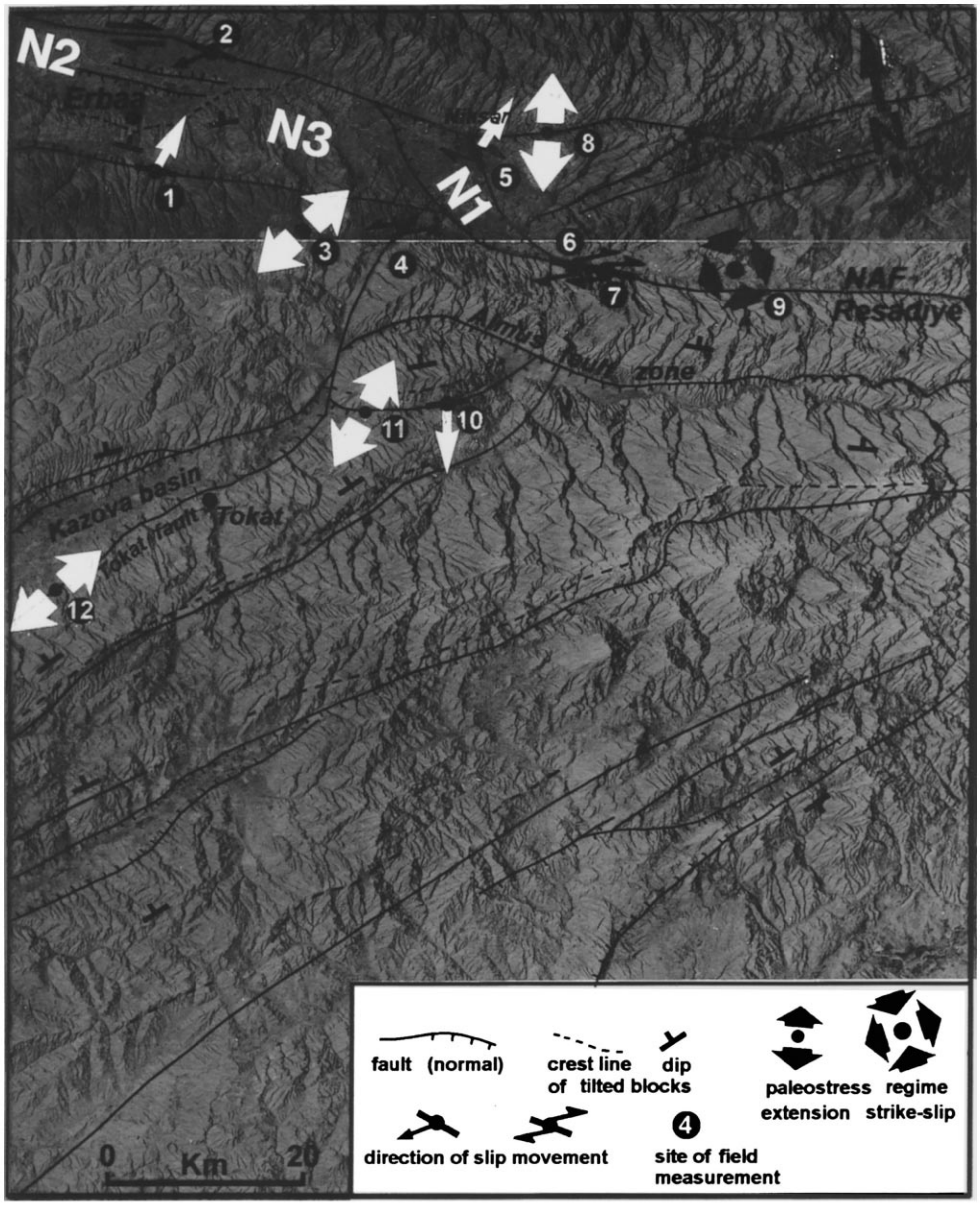

Fig. 3. Interpretation of a mosaic of SAR ERS images (negative view, descending orbit, looking WSW) of the Niksar area (location in Fig. 1c). NAF, North Anatolian Fault. N1, N2 and N3 are Neogene basins. Numbers in circle are sites of structural analysis (see Fig. 4). White and black arrows are slip vectors and extension patterns related to motions, respectively, during the first (late Miocene–early Pliocene) and second (late Pliocene–Quaternary) stages of deformation.

(Dewey et al., 1986; Barka and Kadinsky-Cade, 1988; Reilinger et al., 1997). Analysis of the neotectonics in the Eastern NAF region is consequently critical for the understanding of collision/lateral extrusion relationships.

The NAF has been previously studied with different approaches: geology and geomorphology (Tatar, 1978; Barka and Kadinsky-Cade, 1988), seismology (McKenzie, 1972; Jackson and McKenzie, 1988), aerial photography (Barka, 1992) and Landsat satellite imagery (Suzanne et al., 1990). Synthetic Aperture Radar (SAR) images of the European Remote Sensing (ERS) satellite (ground resolution 12.5 m, wavelength 5.6 cm) and Digital Elevation Models (DEMs) can also provide new neotectonic information because they are sensitive to variations in topographic slope (Chorowicz et al., 1995a). The aim of this paper is to take advantage of the analysis of SAR ERS and DEM imagery and complementary fault analysis in the field, to advocate that extension and strike-slip tectonics prevail in the eastern NAF region, including the Karlıova escape wedge and beyond. We argue that Anatolia is composed of blocks with dimension less than 50 km in width, that are tilted and move relative to each other.

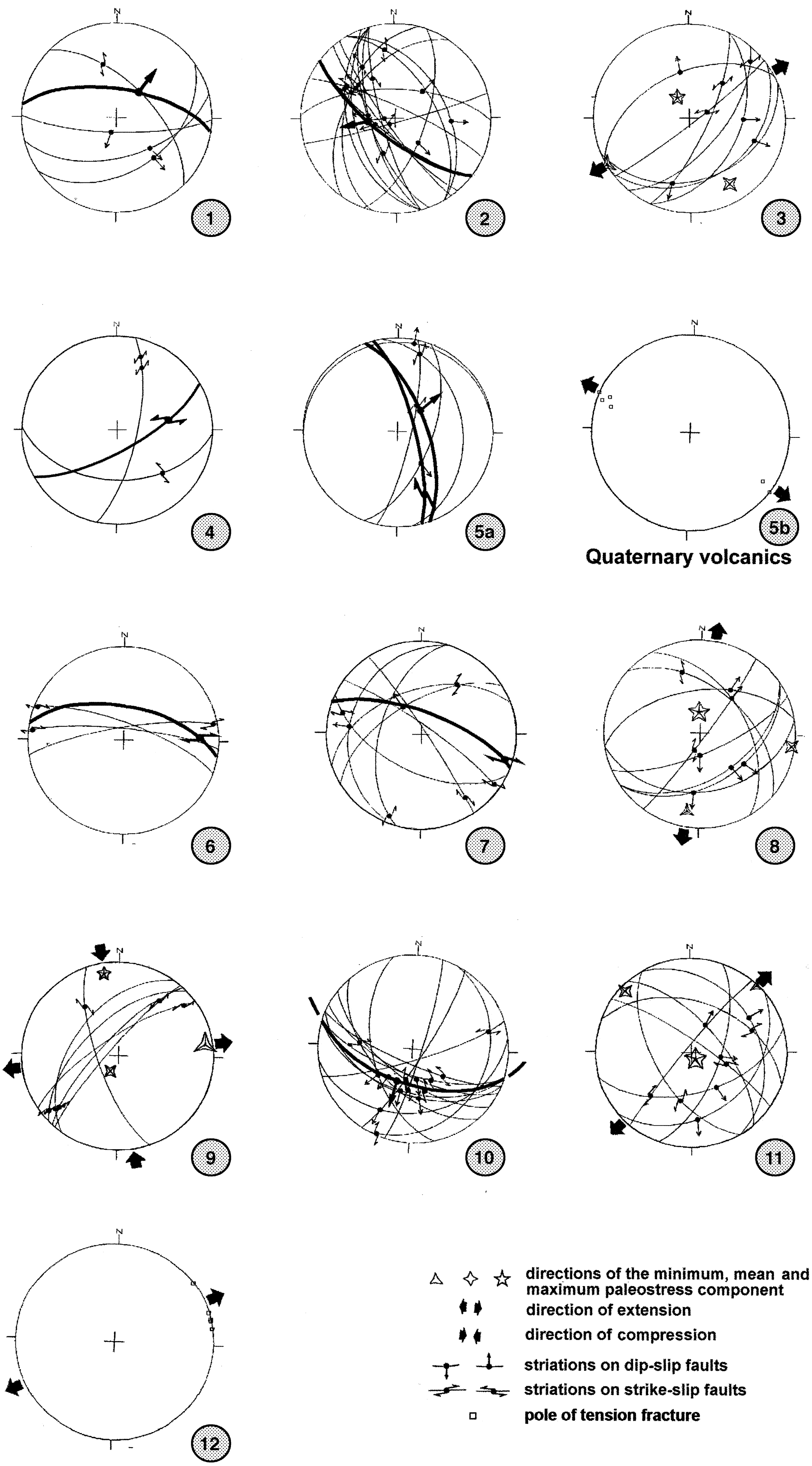

Fig. 4. Stereoplots of field measurements and computed data inversion (Angelier, 1990). Schmidt nets, lower hemisphere. Numbers refer to sites located in Fig. 3. Thick lines and arrows are plots of major (mapped) faults and related striations.

They are compatible with a detachment within the crust of Anatolia.

2. Overview

The DEM image of the studied area (Fig. 1b) shows the Central Anatolia Plateau at a mean altitude of 900 m, located between the Pontides in the north and the Taurus in the south. The NAF is an arched fault zone in plan view, changing strike from N75°E (western NAF) to N110°E (eastern NAF), which reactivates part of the Pontic ophiolitic suture zone (Bergougnan, 1987). According to the bibliographic review made by Barka (1992), offset along the NAF is estimated from 25 km to 350–400 km depending on the authors, and is generally considered to decrease from east to west. Data on the age of the NAF span from the late Pliocene at ca 2.5 Ma (Şaroğlu, 1988; Trifonov et al., 1994), or the early Pliocene at ca 5 Ma (Tatar, 1975; Barka and Hancock, 1984; Barka, 1985; Barka and Kadinsky-Cade, 1988; Koçyiğit, 1989; Barka, 1992; Westaway, 1994) to the late Miocene at ca 12–13 Ma (Dewey and Şengör, 1979; Şengör, 1979; Şengör et al., 1985; Hempton, 1987; Le Pichon et al., 1995). Structural analysis (Suzanne et al., 1990; Barka, 1992) and focal earthquake mechanisms (McKenzie, 1972; Jackson and McKenzie, 1988) indicate that the tectonic regime is strike-slip, accompanied by tension in the western regions. In the curved central part of the NAF a transtensional to extensional regional deformation regime characterized by a SW- to WSW-trending $\sigma3$ has prevailed since the Pleistocene (Bellier et al., 1997).

Crustal movements have been described from Global Positioning System data (Oral et al., 1993; Reilinger et al., 1997). Displacements in Anatolia in the Eurasia reference frame are parallel to the NAF. However, if the Pontic belts located north of the NAF are stable west of Erzincan, they are subject to NNW-directed movement to the east. The displacements we describe in the following are relative west of Erzincan, to the Northwestern Pontides (considered to belong to fixed Eurasia), and east of Erzincan, to the moving Eastern Pontides.

We describe the deformation geometry in the northern region of Eastern Anatolia, between Havza in the west and Karlıova in the east (Fig. 1c). The NAF is composed of Neogene to Quaternary faults (Ambraseys, 1970; Stein et al., 1997) and basins, i.e. from west to east, the Tosya, Ladik, Niksar, Suşehri, Erzincan and Karlıova basins (Fig. 1c). According to Irrlitz (1971), Barka and Hancock (1984) and Barka and Gülen (1988), the basins first developed during the Miocene as post-collisional flysch–molasse depocenters along the Intra-Pontide suture zone. However, most of the fill, composed of lacustrine and fluvio-lacustrine sediments, belongs to the Pontus Formation, which is divided by a Messinian unconformity into the Lower Pontus and Upper Pontus units, dated respectively as Tortonian (12–7 Ma) and Pliocene–middle Pleistocene (5–0.7 Ma) (Irrlitz, 1971; Barka and Hancock, 1984; Barka and Gülen, 1988; Andrieux et al., 1995). On the basis of structural analyses, the Niksar, Suşehri and Erzincan basins have been interpreted in terms of pull-apart structures (Hempton and Dunne, 1984).

Within Anatolia, NE- to E-striking late Neogene faults branch from the NAF (Fig. 1c): the Devrez Çay Fault Zone in the Tosya area (Dhont et al., 1998a), the Almus Fault Zone and other subparallel branches in the Niksar area (Tatar et al., 1995; Bozkurt and Koçyiğit, 1996), the Ovacık Fault in the Erzincan area (Barka and Gülen, 1989; Chorowicz et al., 1995b), and the EAF (e.g. Dewey et al., 1986).

In order to complement our information on the deformation geometry, structural data, which reveal the mechanisms of deformation, were acquired in the field in the west (Niksar) and extrapolated to similar structures in the east. We shall consider that the tectonic mechanisms associated to the Niksar structure are also valid for those located further east.

3. Imagery and field structural analysis

3.1. From Havza to Niksar

Near Havza, the NAF forms a continuous straight N110°E-striking scarp (Fig. 2). Right-lateral displacement is evidenced by a releasing bend basin (Ladik Basin) filled with upper Pontus continental sediments (Irrlitz, 1971). In the southern vicinity of Havza, faults occur with a strike parallel to the NAF (Figs. 1 and 2). The rhomb-shaped Suluova Basin, filled with Quaternary sediments, is bounded by normal faults. Normal faults are recognized by geomorphic characteristics: (1) they are not related to recent drag folds, forming dome-shaped hills, which may have accompanied reverse faulting, (2) instead, they bound tilted plateaus (tilted blocks), and (3) they have a concave trace towards the basin. The Suluova basin can be interpreted as a pull-apart structure.

The Erbaa–Niksar Basin (Figs. 1 and 3) is composed of three sub-basins (N1, N2 and N3, Fig. 3). N3 is composed of deeply eroded Lower Pontus (Tortonian) sediments (Irrlitz, 1971). N2 forms lower plains, cut by a N110°E-trending horst, and is bordered in the north by the active NAF. N2 and N3 have been interpreted as ancient pull-apart basins initiated along the NAF during its early history (Hempton and Dunne, 1984). The rhomb-shaped Niksar Basin (N1) filled with Plio-Quaternary sediments (Barka, 1992) is a lower, more subsiding area

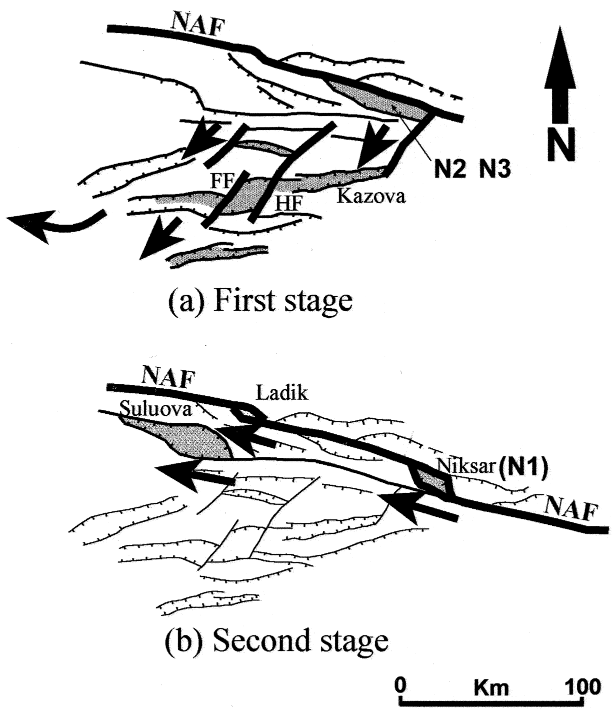

Fig. 5. Interpretation of the late Neogene evolution of the Niksar NAF segment. (a) SW-directed movements in the late Miocene–early Pliocene, forming the N2–N3 and other basins. The overall first stage motion is equivalent to a clockwise rotation shown by curved arrow. (b) WNW-directed motions in the late Pliocene–Quaternary. Very thick lines are faults bounding the deformed area. Other lines are faults, mainly active (thick) or inactive (thin) during the corresponding stage. FF, transfer fault; HF, Hamidiye Fault.

inside a right-stepping relay zone of the NAF. N1 is considered as an example of an active 'lazy Z' shaped basin by Mann et al. (1983), and as a pull-apart basin by Tatar et al. (1995). To the east, a narrow N115°-trending rectilinear valley expresses the Reşadiye segment of the NAF. There are no noticeable deposits in this valley except landslides in places.

South of the Havza and Erbaa–Niksar basins (Figs. 1 and 3), several blocks, tilted north or south, form a pattern of basins and ranges. The main faults strike N75°E, i.e. parallel to the western NAF. According to Tatar et al. (1995), some of these faults may be reverse but they are not related to recent drag folds, forming dome-shaped hills, and instead they bound tilted surfaces. The tilted blocks are expressed on the SAR images by asymmetrical ridges separating opposite parallel type drainage systems (see for example east of the Kazova Basin, Fig. 3). We have systematically compared our images with geological maps in order to carefully separate the scarps formed by fault planes (active) from those resulting from differential erosion of contrasted lithology (ancient). The early Pliocene (Bozkurt and Koçyiğit, 1996) Kazova Basin is elongate and terminates in the east against a NNE-striking fault. This geometry, complemented by observation of tension fractures filled with Neogene sediments along the Tokat Fault at site 12, suggests that the basin was initiated by motion subparallel to the NNE-striking fault. To the west (Fig. 2), normal faults bordering the Kazova Basin are offset by a transfer fault (the Hamidiye Fault) and terminate against the FF fault, which both strike N to NNE. Interpretation in terms of NNE-striking transfer faults implies south-south-westward motion.

To test this interpretation, field structural analysis has been carried out in the Niksar area (Figs. 3 and 4). The strike of tension fractures and the orientation and sense-of-displacement of striated fault planes were measured. Fractures were observed in the Plio-Quaternary clay or unconsolidated conglomerate. Only a few measurements were taken in other rocks. In these cases, measurements of striations were made along open faults filled with clay and breccias that we attributed to the Neogene. Special emphasis was placed on striations directly observed on the major (mapped) fault planes, on which the main part of the regional displacements occurred. When the major fault slickensides could not be observed, striations observed on nearby smaller faults paralleling the major fault were taken into account, assuming that in a given local stress field, parallel faults have the same mechanism, for a given tectonic phase. In Fig. 3, we have plotted on the trace of the main faults, the plunge direction of striations, with indication of the sense of movement. In a few sites, not located along mapped faults, we have used striations on the various minor fault surfaces to estimate the orientation of the local palaeostress tensor as performed by Angelier (1990).

All our measurements indicate extensional or trans-tensional deformation. There are two clearly distinct directions of displacement or stress orientation.

1. Along the main segments of the NAF, at sites 2, 6 and 7, striations are that of displacement oriented approximately east–west. At site 4 along the NNE-striking fault that easterly bounds the Kazova Basin, motion is E–W. At site 9 located apart from the NAF fault line, the stress regime is strike-slip with $\sigma 1$ and $\sigma 3$ horizontal, $\sigma 3$ trending N85°E.
2. At sites 1 and 3, a southern segment of the NAF exposes NE–SW to NNE–SSW displacement testified by striations along the main WNW-striking fault. Such motion orientation is also shown at sites 10 and 11 along an E–W fault located south of the NAF. At site 12, tension fractures along the Tokat fault are indicative of a N70°E extension. At site 8, $\sigma 3$ trends N–S.
3. At site 5, located along the N160–170°E major fault which bounds the Niksar (N1) pull-apart basin to the east, we have observed the two directions, trending N40°E or N160°E (diagram 5a of Fig. 4).

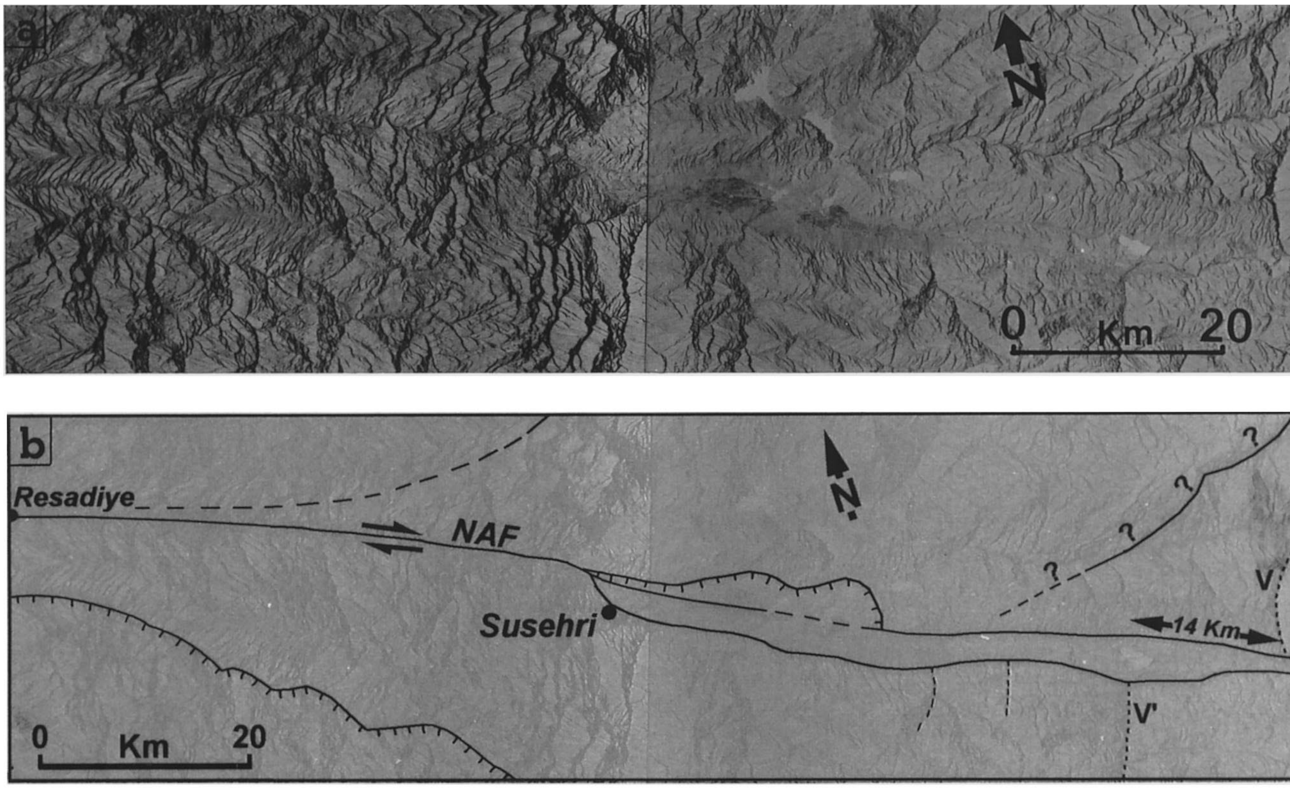

Fig. 6. (a) Mosaic of SAR ERS images (negative view, descending orbit, looking WSW) of the area of Suşehri (location in Fig. 1c). (b) Interpretation of (a). Dashed lines are inferred faults. Question marks: the scarp may be a fault or more simply result from erosion of contrasted lithology. V and V′ are deep valleys laterally displaced (14 km) by the NAF.

There is evidence that the NE–SW to NNE–SSW movements have occurred first and were followed by N110°E to N130°E displacements.

1. Older motions: the Erbaa (N2) basin is deeply eroded and clearly older than the Niksar Basin; the southern border of this N2 basin is not reactivated by the NAF which runs uniquely along the northern border; at sites 1 and 3, located on the southern border (Fig. 3) displacements or stress orientation trends NE–SW (Fig. 4).
2. More recent motions: at site 5, N40°E dykes (N130°E directed extension, Fig. 4, diagram 5b) are associated with Quaternary volcanoes (Tatar et al., 1995); the focal mechanism of the December 20, 1942 earthquake (Dewey, 1976) indicates pure N110°E strike-slip motion along the NAF. This succession of two tectonic events is temporally and spatially the same as that described previously, more to the west along the NAF in the Tosya area (Dhont et al., 1998a).

We propose a new interpretation of the local kinematics (Fig. 5). In a first stage (late Miocene–early Pliocene), SW- to SSW-directed extension produced oblique-slip normal faulting (Fig. 5a). The FF, Hamidiye and other NE-striking faults acted as left-lateral transfer fault zones forming the eastern boundary of the deformed area. Extension resulted in transtensional opening of the N3–N2, Kazova and other E–W elongated basins. Normal faulting occurred in both sides of the NAF. In a second stage (late Pliocene–Quaternary), motion turned west-northwestward, more or less parallel to the NAF, resulting in the opening of the Ladik and the Niksar basins (Fig. 5b). The Suluova Basin was formed in the releasing-bend of a former oblique-slip normal fault. This model implies that the NAF was active (transtensional) only west of Niksar in the first stage, and that the deformation subsequently migrated eastward. Transtension accommodated westward movements inside a wedge ending at Niksar, bounded to the north by the NAF, and to the south by NE-striking left-lateral faults. This model is compatible with that presented by Dhont et al. (1997) for the Tosya area (Fig. 1c) and may also be valid for our interpretation of the Erzincan Basin. We could not carry out field structural analysis near Erzincan but we assume that two tectonic events have also occurred there (see below).

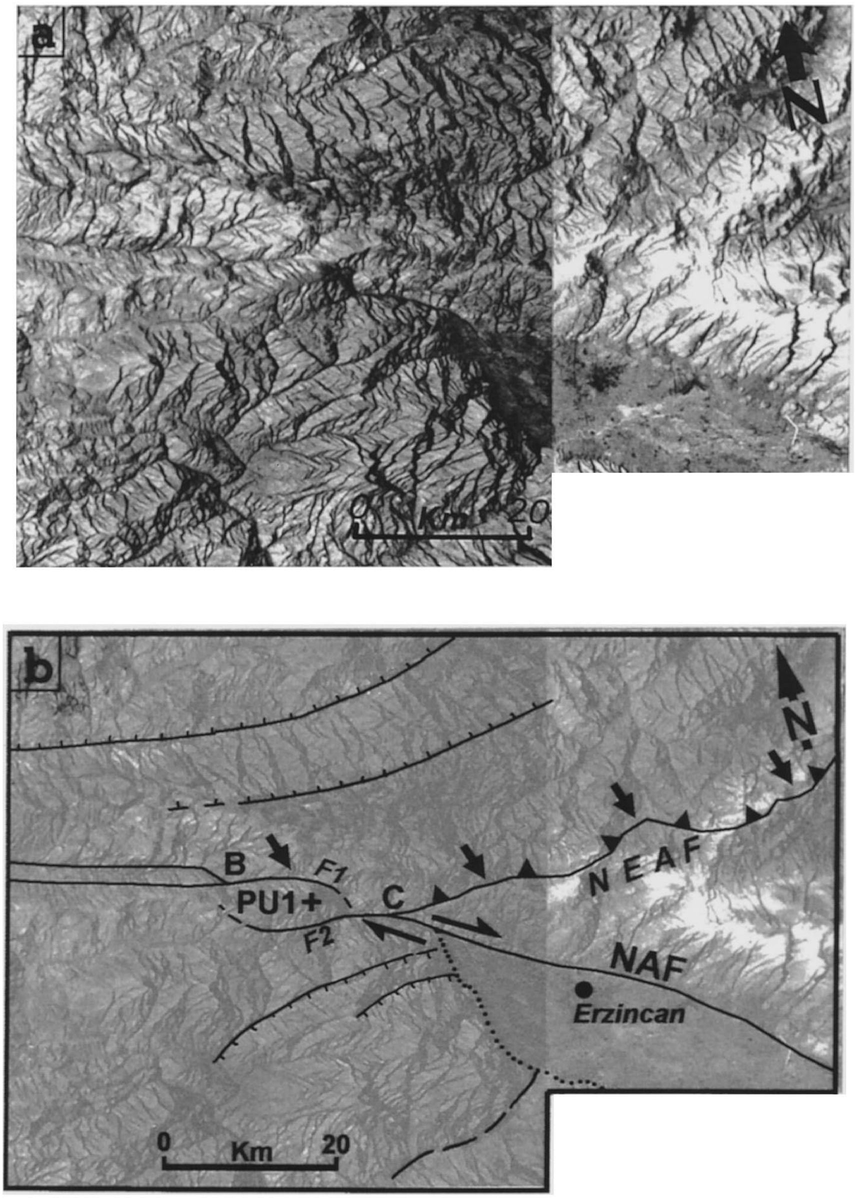

Fig. 7. (a) Mosaic of SAR ERS images (negative view, descending orbit, looking WSW) of the area west of Erzincan (location in Fig. 1c). (b) Interpretation of (a). B, eastern end of a narrow Pliocene basin. C, NAF–NEAF branching. NEAF, Northeast Anatolian Fault. PU1, push-up structure bounded by faults F1 and F2. Arrows: relative motions.

3.2. Suşehri–Erzincan area

In the Suşehri Basin (Fig. 6), early–middle Miocene to Holocene sediments (Koçyiğit, 1989; Barka, 1992) are bordered by normal faults with curved traces. The NAF forms a straight line across the basin infill. To the east, the NAF corresponds to a narrow ($\approx$2 km) elongated (80 km) fault-bounded basin filled with Pliocene sediments, attesting to transtension at that time. The most convenient valleys which can be used for assessment of NAF offsets are those trending N–S, at right angles to the NAF. They are well shown by radar illumination from the east. One of them (V in Fig. 6b) can be correlated on the other side with several valleys of the same width, depth and trend. Correlation with V′ yields a minimum of 14 km dextral displacement.

Beyond the eastern end of the Suşehri Basin (point B in Fig. 7b), the NAF is a unique fault (F1) bounding a block to the northeast with distinct relief (PU1), emphasized by a recently uplifted erosion surface. There is a relay with fault F2 which turns eastward to N120°E and forms the northern boundary of the Erzincan Basin. The relay pattern formed by the F1 and F2—two segments of the dextral NAF—is right-stepping and should theoretically have formed a pull-

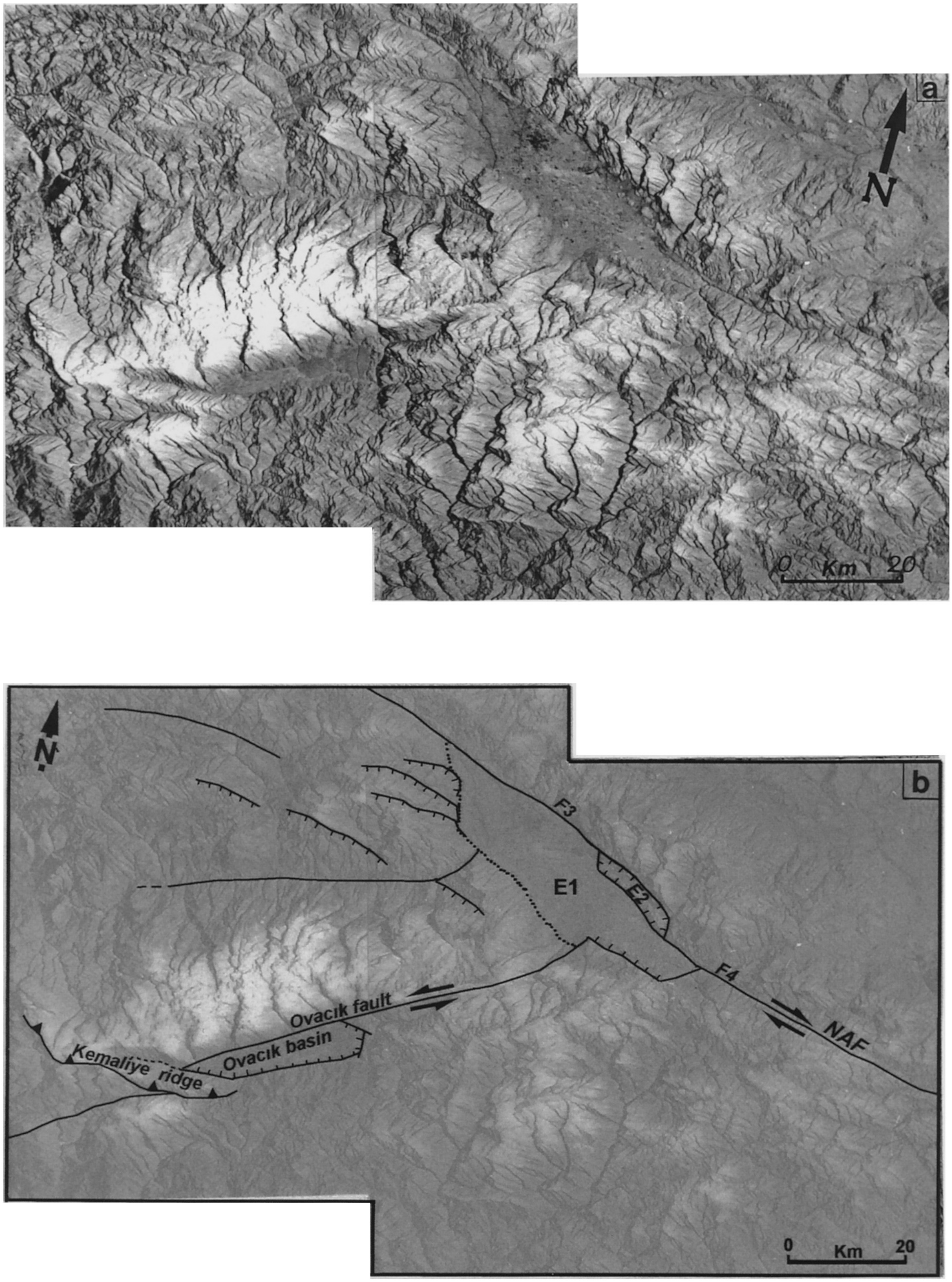

Fig. 8. (a) Mosaic of SAR ERS images (negative view, ascending orbit, looking ENE) of the Erzincan Basin (location in Fig. 1c). (b) Interpretation of (a). E1, main basin formed by a first motion parallel to the Ovacık Fault. E2, minor pull-apart basin formed by a second motion parallel to the NAF. F3 and F4 and F5 are NAF segments.

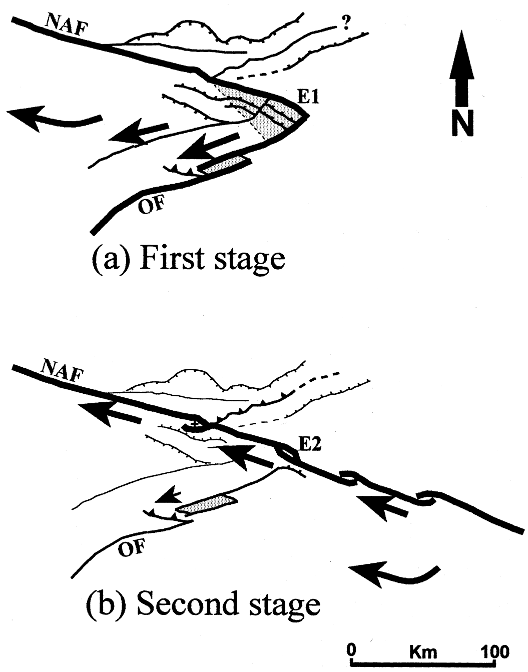

Fig. 9. Interpretation of the tectonic evolution of the Erzincan Basin. (a) Early opening of the E1 basin by SW-directed block motion. This is equivalent to a clockwise rotation that opened the E1 basin. (b) Quaternary dextral transcurrent motion along the NAF, inducing the E2 pull-apart basin and push-up features, together with continuation of westward displacement along the Ovacık Fault (OF).

apart basin instead of the PU1 relief. However, at point C, the NAF connects with the North East Anatolian Fault (NEAF), a fault with a south-verging thrust component (Philip et al., 1989; Suzanne and Lyberis, 1992; Lyberis et al., 1992). To explain the uplifted PU1 structure we have to assume that the NEAF is active and that local compression results in a range (Fig. 7b).

The Erzincan Basin is filled with Plio-Quaternary sediments (Irrlitz, 1971; Barka, 1992) and is bounded to the northeast by a continuous succession of faults (Fig. 8). The major one (F3 in Fig. 8b) is the southeastern continuation of the NAF, but to the east it becomes curved in plan view. To the east, another fault (F4) continues in the N110°E direction as the main NAF. The relay zone (E2) is a narrow rhomb-shaped low plain exposing several volcanic cones of Quaternary age (Hempton and Dunne, 1984). E2 is distinct from the largest main Erzincan Basin (E1). The southwestern border of E1 is not bordered by large faults but rather by a topographic flexure and a discontinuous line of small normal faults. Several faults can be mapped from the SAR images in the area northwest of the basin.

The southern corner of the Erzincan Basin is connected with the Ovacık Fault. From offset of the Euphrates River and estimate of the shortening in the Kemaliye Ridge (Chorowicz et al., 1995b), the finite sinistral strike-slip displacement along the Ovacık Fault is $\approx$12.5 km. Part of the movement occurred in the late Quaternary, as attested by the Ovacık Fault cutting alluvial fans and glacial deposits (Arpat and Şaroğlu, 1975).

Several interpretations of the formation of the Erzincan Basin have been proposed. According to Hempton and Dunne (1984), the basin is a simple pull-apart feature. For Barka and Gülen (1989), west-directed movements of the Anatolian plate occurred in two stages, both in the E–W direction: (1) opening of a 'releasing double bend' basin along the NAF; and (2) formation of the Ovacık Fault and widening of the basin. Our interpretation also considers two steps (Fig. 9) but with different directions in block movements, and is coherent with the tectonic model we have proposed for the Erbaa–Niksar area (Fig. 5). In the Pliocene, the first motion was with motion trajectories turning in space from SW—parallel to the Ovacık Fault, to WNW—parallel to the NAF (Fig. 9a). This block rotation resulted in the opening of the E1 Erzincan Basin. This clockwise block rotation is necessary to explain why the E1 basin progressively closes in the west. Extensional faulting inside the moving blocks, west of the basin, compensated the opening. In the Quaternary, the movement orientation changed to N110°E, resulting in the right-lateral opening of the E2 pull-apart basin, giving way up to the magma (Fig. 9b).

In the Erzincan region, extension tectonics also occurred north of the NAF (Fig. 1). Faults bordering elongate tilted blocks have curved traces in map view and bound topographic depressions which contain late Neogene sediments, such as the Kolkit Basin. It is important to emphasize that extension may occur in the Pontides, outside of Anatolia.

3.3. *Tanyeri–Karlıova area*

Southeast of the Erzincan Basin, the NAF is a straight, discrete scarp striking N110°E (Figs. 8 and 10). Near Tanyeri, a 6 km long push-up range (PU2) is related to a left-stepping fault relay. To the east, the Yedisu elongate basin has been interpreted as a pull-apart structure (Barka and Kadinsky-Cade, 1988). SAR imagery shows that this basin extends further northwest into narrow, low areas devoid of sediments. This graben is followed easterly by a fault segment and a left-stepping relay zone forming a distinct 15 km long ovoid ridge, which we interpret as a push-up swell (PU3).

In the Karlıova area, SAR ERS and SPOT images (Figs. 11 and 12) show elongate N80°E to N120°E fault-bounded blocks. They are topped by SW-dipping erosion surfaces indicating that they have been recently tilted. The bounding faults are normal because they

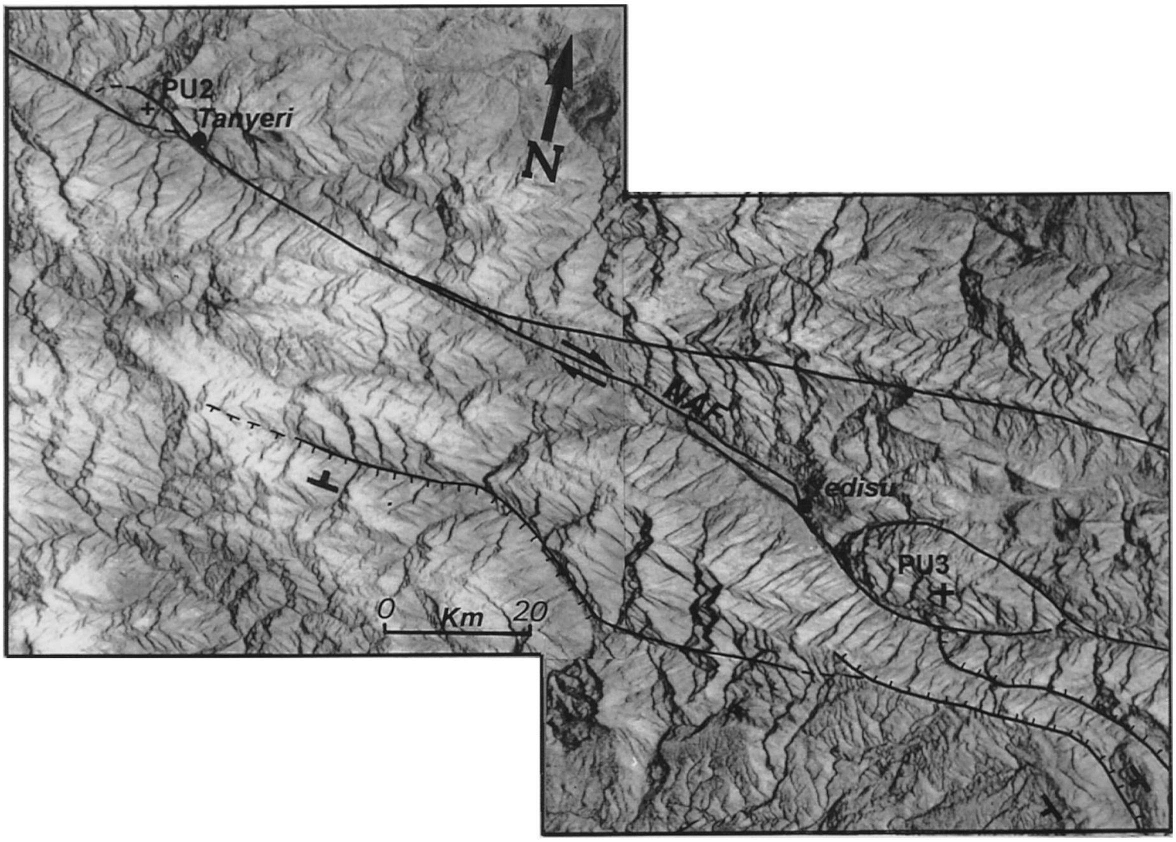

Fig. 10. Interpretation of a mosaic of SAR ERS images (negative view, ascending orbit, looking ENE) of the Tanyeri segment of the NAF (location in Fig. 1c). PU2, PU3, push-up blocks.

displace planar erosion surfaces and have curved fault traces, implying SW-directed extension. Smaller normal faults can be observed inside the blocks. However, focal mechanisms of earthquakes along the NAF attest to strike-slip motion (Jackson and McKenzie, 1984). The presence of extensional type tilted blocks and push-up structures in this area indicates that the nearby segment of the NAF can be transtensional or transpressional depending on the segment considered. Beyond the NAF to the north, we interpret the presence of another ESE-striking normal fault. There is also a large NE-trending sinuous line, visible on Fig. 11(a), which seems to be related to an ancient (late Eocene) structure. The Karlıova Basin, filled with Plio-Quaternary sediments (Dewey et al., 1986) and bounded by the NAF and the EAF, is considered to result from extension. This is consistent with the opinion of several authors (Şengör, 1979; Şengör et al., 1985; Dewey et al., 1986; Pasquarè et al., 1988; Tutkun and Hancock, 1990) who have advocated extension in the Karlıova area, but contrary to others (Barka and Gülen, 1988; Yılmaz, 1993) who have argued compression. From a topographic map, we have drawn a balanced cross-section along a line parallel to the EAF (Fig. 12b). Estimate of the finite displacement projected along the N110° strike of the NAF is 2 km.

At the southern boundary of the Karlıova Basin, the EAF forms a unique line. To the south it passes along the strike to a complex Riedel type fault zone attesting to left-lateral strike-slip movement (Figs. 11 and 12). We infer from this pattern that block movement is SW-directed. Inside the NAF–EAF wedge (Fig. 12a) the fault-bounded blocks are tilted to the southwest. Two major faults have arched traces with concavity to the southwest. In map view the swarm of block faults diverge southeastward. This pattern can be explained by clockwise rotation of the blocks, implying that local motion turns in space from SW to W (Fig. 12c). This model is very similar to that presented in Fig. 9 for the first opening of the Erzincan Basin.

The Karlıova area is generally considered as the eastern end of the Anatolian plate at the NAF–EAF junction (e.g. McKenzie, 1972; Le Pichon et al., 1995). The EAF is interrupted but the NAF continues eastward for 60 km, forming the Varto Fault Zone (Ambraseys and Zatopek, 1968; Tchalenko, 1977), in which faults are curved in plan view. We consider these faults as normal and not reverse, contrarily to Şaroğlu and Yılmaz (1989), because the fault scarps separate tilted planar surfaces, typically a system of

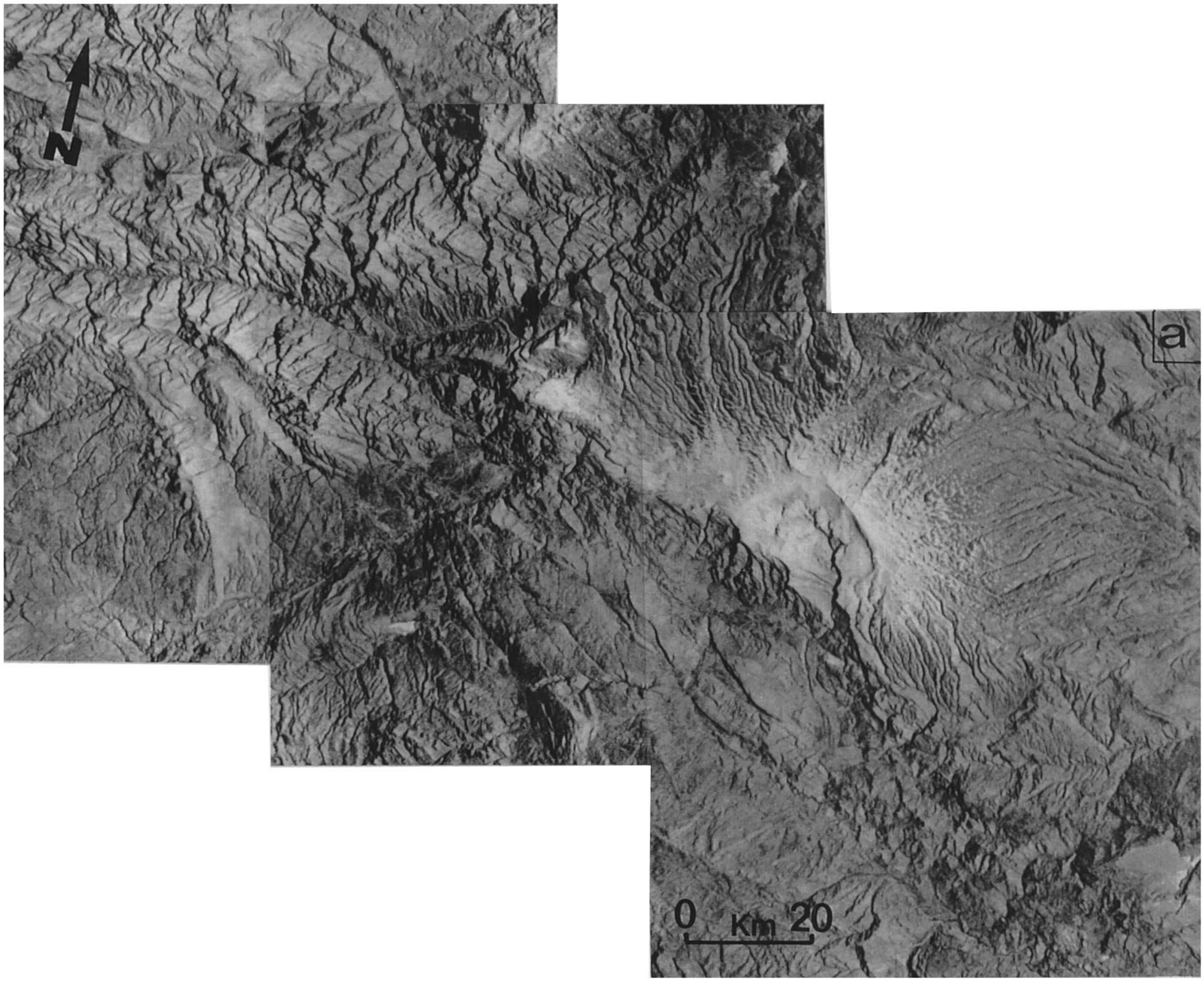

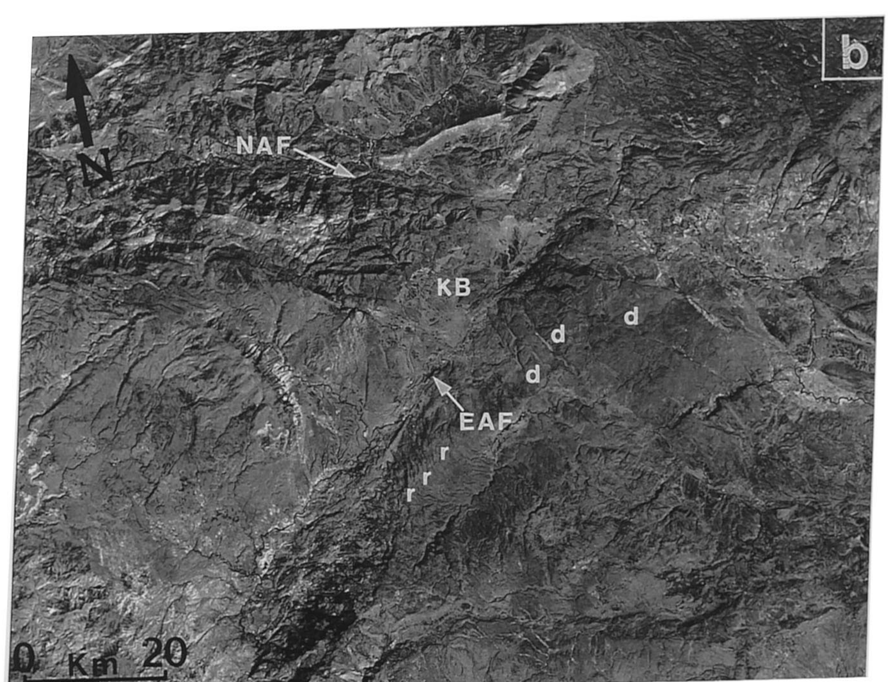

Fig. 11. (a) Mosaic of SAR ERS images (negative view, ascending orbit, looking ENE) of the Karlıova area (location in Fig. 1c). (b) SPOT image of the Karlıova area (location in Fig. 1c). d, dykes; EAF, East Anatolian Fault; KB, Karlıova Basin; NAF, North Anatolian Fault; r, Riedel faults.

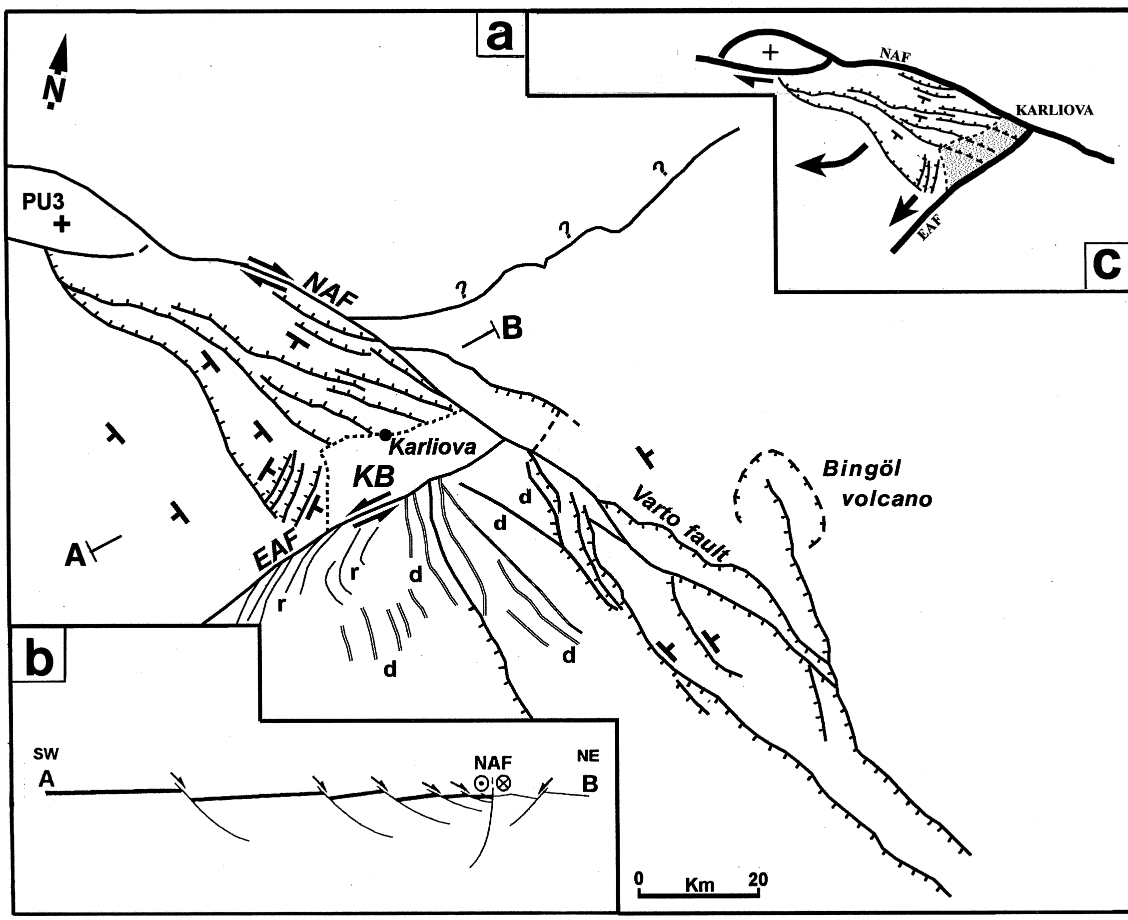

Fig. 12. (a) Interpretation of Fig. 11(a and b). d, dykes; EAF, East Anatolian Fault; KB, Karlıova Basin; NAF, North Anatolian Fault; PU3, push-up structure; r, Riedel faults. T represents dip and strike of tilted block. Circular line, caldera of Bingöl Dag volcano. AB, location of cross-section presented in Fig. 12b. (b) NE–SW cross-section accounting for 2.7 km of extension. This is equivalent, along the NAF trend (N110°E), to a maximum displacement of 2 km for the main block containing point A, taking block rotation into account. (c) Scheme illustrating the opening of the Karlıova Basin. Combined transcurrent motions along the NAF and the EAF, together with variable extension within the Karlıova wedge are equivalent to clockwise rotation.

tilted blocks. Reverse faults however would have been associated with drag folds affecting the erosion surface on top of the blocks. This extensional behaviour is confirmed east of Karlıova by clear occurrences on the satellite images (Fig. 11) of NW-striking dykes, also mentioned by Yürür et al. (1998) on the basis of aerial photography analysis. In this area, Ambraseys and Zatopek (1968) and Wallace (1968) have reported large open fractures in volcanic rocks of the upper Miocene–Pliocene Bingöl formation (Pearce et al., 1990; Şaroğlu and Yılmaz, 1991). Tutkun and Hancock (1990) have shown well exposed truncated ridge spurs (triangular facets) reflecting recent normal fault motions. Some of their mapped faults correspond to the dykes which we have observed on the satellite images. From SPOT, we have mapped one of the dykes continuing southeastward into a normal fault scarp (Fig. 11b and Fig. 12c).

According to Barka et al. (1987), the focal mechanisms of the 1966 earthquakes which occurred along the Varto Fault Zone indicate dextral transpressive motion, related to N-trending compression, but for Wallace (1968), surface fracturing is indicative of a normal component. Ambraseys and Zatopek (1968) shared the opinion of Wallace (1968) and argued that the Varto earthquake of 1966 was mainly associated with dextral movements along $\approx$N125°E fractures associated, or not, with normal components that are predominant by places. Tutkun and Hancock (1990) gave other field observations in the Karlıova area arguing that the NAF experienced right-lateral oblique-slip motion, while the EAF was subjected to left-lateral oblique-slip normal displacements. Şaroğlu (1988) and Şaroğlu and Yılmaz (1991) have indicated that southern blocks were down-thrown with respect to the northern ones, but did not present any arguments as to whether the slip was reverse or normal. Adıyaman et al. (1998) have studied the region east of Karlıova and found strike-slip deformation but no clear reverse faults, and no folds. We interpret this contradictory

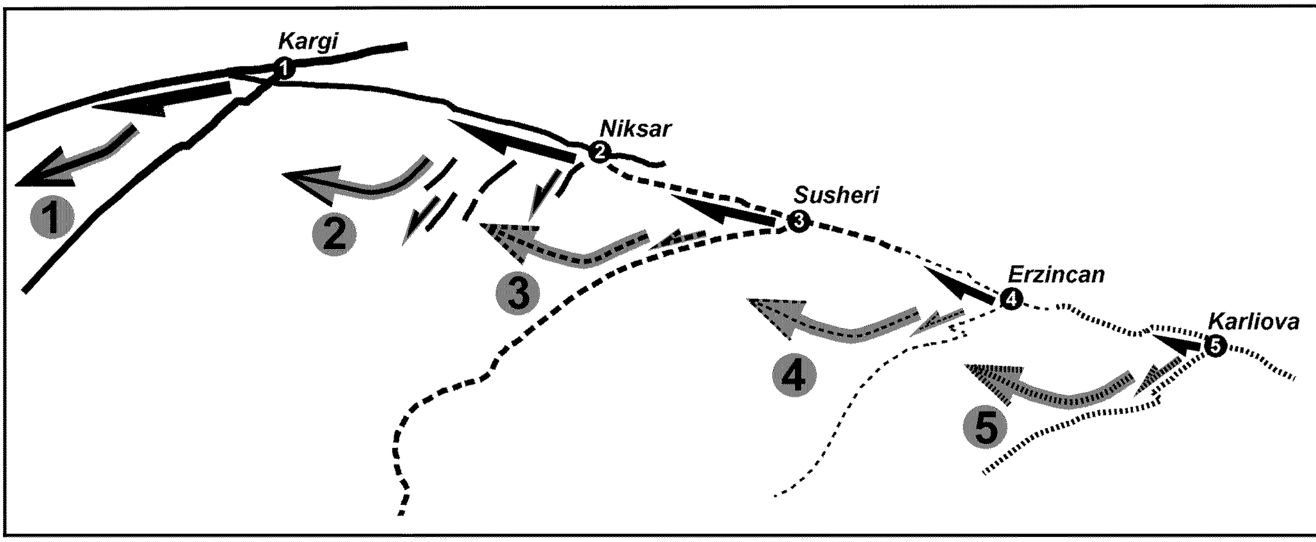

Fig. 13. Model of propagation of the active NAF from west to east. Black circles are inferred successive positions of the wedge head. Corresponding fault systems and block rotations (curved arrows) are displayed by different dashed or continuous lines. Straight arrows indicate inferred transcurrent motion variations along the NAF.

set of arguments to be the result of local compression and extension along different fault sections in a strike-slip regime.

4. Discussion

4.1. Migration of the escape wedge from west to east

Analogies in the structures at Tosya–Kargı (Dhont et al., 1998a), Niksar, Erzincan and Karlıova are striking, and can be explained by the same model (Fig. 13). Inside a given wedge formed by the NAF and a NE- to ENE-striking fault zone, the first motion is directed WNW to SW, and results in the formation of a basin inside the fault corner. In the meantime, to the west the motion is directed WNW to W, parallel to the NAF. Afterwards, in a second stage, at the same location, WNW- to W-directed motion occurs. For instance at Karlıova, the first phase has just been achieved. At a given location, during the first stage, tension affects an area larger than the corresponding wedge, resulting in the formation of subsiding structures also located north of the NAF and east of the NE-striking fault (e.g. the EAF). On the basis of paleomagnetic data, Tatar et al. (1995) have proposed anticlockwise rotation of small blocks in a first stage (late Pliocene), followed by generalized westward motion of the Anatolian plate in a second stage (Plio-Quaternary). Our map has similarities with those of Şengör and Barka (1992), Tatar et al. (1995) and Bozkurt and Koçyiğit (1996), which point out splays of E- to NE-striking faults branching to the NAF.

The EAF is considered as the present-day eastern boundary zone of the Anatolian lateral expulsion. We suggest that this role was formerly played, in the studied area, from west to east, successively by the Devrez Çay Fault Zone (Dhont et al., in press b) near Tosya, the Suluova–Tokat Fault Zone near Niksar and the Ovacık Fault Zone near Erzincan. Each of these fault zones extends far (100 km or more) to the south across the Anatolian Plateau. It is relevant that total displacement along the Ovacık Fault is $\approx$12.5 km, quite similar to that of the paralleling EAF (20 km according to a structural analysis of Dewey et al., 1986). Our model implies that the escape wedge has propagated from west to east by successive jumps (Fig. 13). The escape wedge was first at Kargı, then jumped to Niksar, subsequently to Erzincan and then finally to Karlıova. Prolongation of the NAF beyond Karlıova along the active Varto Fault and extension east of the EAF suggest that eastward propagation is ongoing.

Jackson and McKenzie (1984), in questioning whether Central Anatolia can be considered as a rigid block, envisaged a progressive jump of the EAF eastward to help prevent crustal thickening. However, our model of propagating escape wedges by successive jumps is hard to explain in the simple frame of lateral extrusion of a rigid block, connected with the Arabia/Eurasia collision and related to relative Africa/Arabia transcurrent motion along the Dead Sea fault system. Another dynamic process, independent from Arabia/Eurasia collision and Africa/Arabia transcurrent motion, may be responsible for these tectonics; possibly the Aegean extension occurring further west, combined with buoyancy forces arising from crustal thickness contrast. The pull of the African plate along the Hellenic Trench is responsible for the deformation

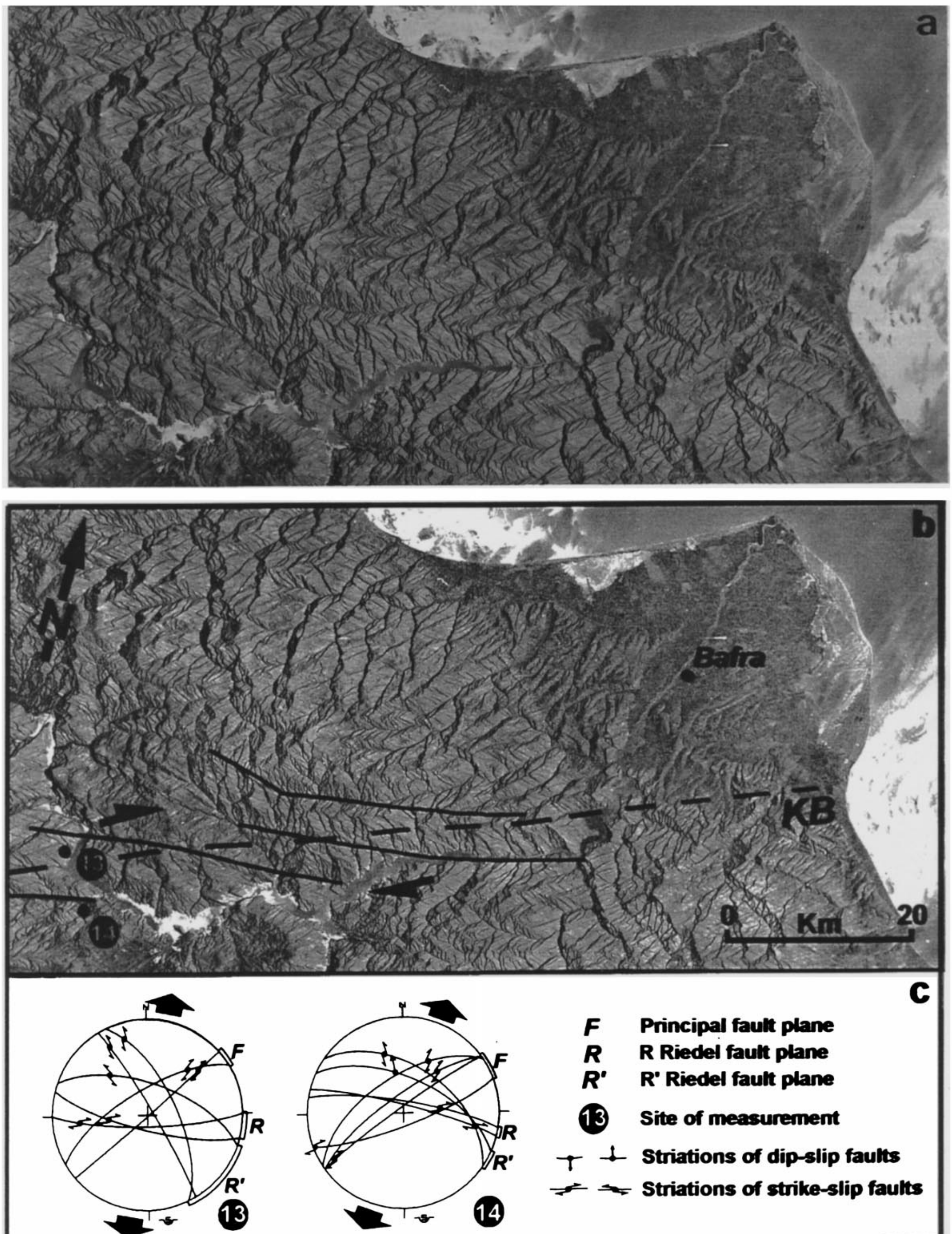

Fig. 14. (a) SAR ERS image (negative view, ascending orbit, looking ENE) of the Bafra region (location in Fig. 1c). (b) Interpretation of Fig. 13a. The Kargı–Bafra Fault Zone (KB), which was detected on the DEM of Fig. 1b, corresponds to en échelon faults interpreted as Riedel patterns. (c) The field structural analysis in sites 13 and 14 is displayed on Schmidt nets, lower hemisphere. We have recognized Riedel systems with, F, the principal fault planes (dextral), and R and R′, respectively the additive (dextral) and subtractive (sinistral) Riedel faults. Extension trends N10°E in site 13 and N20°E in site 14.

in the Aegean and Western Anatolia (Reilinger et al., 1997), and may play some part in the pattern of deformation as far as central and eastern Anatolia. McKenzie (1972) thought that the present westward motion of Turkey relative to Eurasia could be maintained by the potential energy differences between the thick crust in eastern Turkey and the Caucasus, and the low elevations of the Aegean and western Mediterranean.

Our model implies clockwise rotation of crustal blocks. Such clockwise rotation has also been considered by Şengör et al. (1982) and Jackson (1994). For Şengör et al. (1982), the westward motion of Anatolia relative to Eurasia is taken up by fault splays which are similar to those described in this paper, and which may account for an apparent westward decrease in displacement on the NAF. This is inconsistent with our displacement estimates which show an eastward decrease in the offset of NAF. For Jackson (1994), the relative motion between Arabia and Eurasia might have induced clockwise rotation along fault splays parallel to the EAF, thereby decreasing the angle between the NAF and the EAF through time and reducing the surface of the escaping Anatolian block. We show, on the contrary, that extension associated with strike-slip displacements prevails in Eastern Anatolia, extending the surface occupied by the fault-bounded blocks. Moreover, we show that the set of parallel faults began to be active diachronously from west to east, and not synchronously as would be the case for the model of Jackson (1994).

The model of propagation of escape wedges by successive jumps is supported by other evidence. According to Şaroğlu (1988) and Trifonov et al. (1994), the NAF was initiated in the late Pliocene at ca 2.5 Ma by the linkage of several pre-existing segments. The propagation was supposed to occur from east to west (Barka and Gülen, 1988; Barka, 1996). However, Westaway (1994) concluded from kinematic data that the rate of displacement along the NAF is higher in the west than in the east. This is consistent with the following evidence showing that the NAF is older in the west. Arger et al. (1996) and Westaway and Arger (1996) suggest that: (1) from ca 5 to ca 3 Ma, the Turkish–Arabian plate boundary was the Malatya–Ovacık Fault Zone, the NAF ending at Erzincan; and (2) that the EAF has formed only since ca 3 Ma, or even later at ca 2 Ma (Şaroğlu and Yılmaz, 1991; Yürür and Chorowicz, 1998). Basing their opinion on the observation that shorter traces of the faults compose the NAF near Karlıova, Tutkun and Hancock (1990) concluded that the youngest NAF segment lies in this region.

However, this model is in conflict with several other authors, e.g. Barka (1992) estimated a 40 ± 5 km finite displacement in the west and 25 ± 5 km in the east. According to Hempton (1982) the eastern NAF is older and extended as a straight trace to the Black Sea, whereas the western NAF is younger and was left-lateral before the occurrence of a strike-slip reversal of the displacement in the Plio-Pleistocene. According to Suzanne et al. (1990), propagation was first from Karlıova along a N125°E strike, up to the Inebolu–Havza segment then, after blockage against the Black Sea oceanic crust, propagation was westwards, following a N75°E strike.

The DEM (Fig. 1b and c) suggests that the western NAF extended east of Tosya up to the Bafra peninsula. The DEM feature is that of a unique line (Kargı–Bafra line, KB line). On the SAR image (Fig. 14) we have mapped en échelon faults compatible with an overall dextral displacement. To check this interpretation we have searched for fault traces in the field. Outcrops of low-grade metamorphic rocks of the Permo-Triassic Karakaya complex (Okay, 1989) are well exposed all along the main road cutting the fault line. Neogene fractures have been found only in sites 13 and 14 (Fig. 14b and c), i.e. right on the KB line. The fractures are open faults with gaps up to several metres wide, filled by yellowish clay and breccias similar to that of the Neogene. The fracture pattern in each site can be interpreted as a Riedel system compatible with dextral oblique-slip displacement along the KB line (Fig. 14c). The N10°E to N20°E extensions are parallel to the first movements that we have observed in the escape wedges of the other regions.

Our estimates of finite displacements are 14 km (at least) west of Erzincan and 2 km at Karlıova. We interpret an eastward decrease in strike-slip finite motions along the NAF. While blocks move southwestward, they also extend and occupy the increasing surface within the escape wedges.

Volcanic activity has been widely developed in Anatolia since the Neogene. It has generally given rise, during the initiation phases, to large volumes of calc-alkaline products and has evolved into alkaline rocks throughout Anatolia during the latest stages (Pearce et al., 1990; Yılmaz, 1990; Güleç, 1991; Seyitoğlu and Scott, 1992). The geochemical evolution of the volcanic products with time is similar to that reported from the Basin and Range and the Rio Grande Rift in the USA (e.g. Dungan et al., 1986; Fitton et al., 1991). The volcanic activity appears to have started in the late Oligocene–early Miocene in Western Anatolia (Seyitoğlu and Scott, 1992; Gündoğdu et al., 1994), middle Miocene in Central Anatolia (e.g. Temel, 1992) and late Miocene–Pliocene in Eastern Anatolia (Pearce et al., 1990).

Volcanic activity with similar geochemical evolution has also developed along the NAF, initiating from west to east successively around the Kızılcahamam–Cerkes, Niksar–Reşadiye and Erzincan areas (Keller et al., 1992; Gündoğdu et al., 1994), with the initial volcanism respectively dated early Miocene, late Miocene and Pliocene. These data concur to show that the extension first started in Western Anatolia and propagated through time along the NAF to reach the Eastern Anatolia region.

4.2. Crustal detachment in Anatolia

Most authors (e.g. McKenzie, 1972; Dewey, 1976; Westaway and Arger, 1996) have considered the EAF as a plate boundary but others (Şengör et al., 1985; Dewey et al., 1986), estimating total slip along the EAF, have suggested that it cannot be a transform zone.

The model of escape wedges propagating from west to east with successive jumps of fault zones parallel to the EAF implies that the EAF can hardly be a plate boundary because otherwise each of the faults similar to the EAF would be a plate boundary. Anatolia is consequently not a simple individual plate. We have shown that the first motions inside a newly-forming escape wedge are directed SW, i.e. not parallel to the NAF, and afterward move to the west. Following the view of McKenzie and Jackson (1983), the rotating blocks are upper crust rigid blocks. Indeed, Anatolia is formed of elongate units with crustal block dimensions of less than 50 km wide and several hundred kilometres long. Along the NAF and in Central Anatolia earthquakes are restricted to shallow levels, the deepest earthquake foci reaching 13 km in the central part of the NAF (Jackson and McKenzie, 1984), and no more than 15 km in Eastern Turkey, as noticed by Yılmaz (1990). This suggests that the faults affect the crust and not the brittle lithospheric mantle.

Most of Western to Central Anatolia (including the area immediately east of Karlıova) is experiencing extension. Compression may occur locally, e.g. in the Tosya (Andrieux et al., 1995) and the Sivas basins (Poisson et al., 1992) or in the push-up structures along the NAF. Local compression in a general context of extension is likely to occur occasionally at the boundary of crustal blocks which move more or less independently over a detachment zone.

Our interpretation is that after a jump of the escape wedge, the movement of blocks near the new southeastern wedge boundary is first directed SW, and then turns to the west (Eurasia being considered fixed) and is not contradictory with a more general W- to WNW-directed motion of Anatolia shown by the GPS data (Oral et al., 1993; Reilinger et al., 1997). There is no contradiction especially if motions of the Eastern Pontides and Eastern Turkey relative to Eurasia are taken into account. In our model, each Anatolian crustal block moves relative to its neighbours and they all move together relative to Eurasia along the NAF and the EAF. This resembles a plate motion. However, since in our hypothesis the southeastern boundary of Anatolia migrates eastward through time, we suggest that the lithospheric mantle of Anatolia does not behave like a simple individualized plate but is subjected to westward ductile extension.

From these arguments, we conclude that the deformation in Anatolia is principally that of crustal blocks which are detached at the brittle–ductile boundary within the crust. The late Neogene history of this region began by extension in the Aegean region in the early Miocene (Altherr et al., 1982; Gautier et al., 1990), inducing a detachment of the Western Anatolian crust. Extension progressively propagated to the east up and beyond Karlıova. This is however compatible with the model of collision responsible for lateral extrusion of a rigid plate.

5. Conclusions

Using radar and DEM imagery, we have described new local tectonic features along the Eastern NAF: (1) a releasing bend Quaternary basin (Ladik Basin); (2) the rhomb-shaped Suluova Basin, interpreted as a pull-apart structure opened by right-lateral strike-slip along N95°E striking faults; (3) normal faults bordering the Kazova Basin, offset by a dextral NNE-striking transfer fault; (4) north of the NAF, late Neogene N110°-striking faults having normal slip components; and (5) the NEAF activity at the point where it branches with the NAF.

The main results of this study concern large-scale tectonics.

1. Extension and transtension have prevailed since the late Neogene along the NAF in Eastern Anatolia, including the Karlıova triangle and beyond.
2. The Anatolian region is composed of blocks with dimension less than 50 km in width, that are tilted and move relative to each other. They are compatible with a detachment within the crust of Anatolia.
3. The escape wedge has migrated by successive jumps from west to east, creating fault zones parallel to the EAF.
4. In each escape wedge, SW-directed movements predate strike-slip tectonics along the NAF. This view is valid for the Tosya, Niksar, Erzincan and Karlıova wedges.
5. The lithosphere of Anatolia is subjected to extension. This is not the behaviour of simple lateral extrusion induced by forces applied at the boundaries of the Anatolian lithospheric block by the Eurasian and Arabian adjacent plates, but rather the configuration of regional extension due to backward retreat of the Hellenic slab and buoyancy forces arising from crustal thickness differences (Dewey, 1988).
6. Crustal blocks move southwestward and extend at the same time in order to occupy the increasing surface within the escape wedges.

Acknowledgements

This work has been funded by both the French CNRS (project PICS) and the Turkish TUBITAK (project YBAG-0078/DPT), with support from the French Embassy in Ankara and the Ministère des Affaires Etrangères in Paris. ERS radar data were provided by the European Space Agency (project AO.F7) and processing expenses were partly supported by the Centre National d'Etudes Spatiales. We are grateful to two anonymous reviewers for valuable comments and suggestions that largely improved the quality of the manuscript.

References

Adıyaman, Ö., Chorowicz, J., Köse, O., 1998. Relationships between volcanic patterns and neotectonics in Eastern Anatolia from analysis of satellites images and DEM. Journal of Volcanology and Geothermal Research 85, 17–32.

Altherr, R., Kreuzer, H., Wendt, I., Lenz, H., Wagner, G.A., Keller, J., Harre, W., Hohndorf, A., 1982. A late Oligocene/Early Miocene high temperature belt in the anti-cycladic crystalline complex (SE Pelagonian, Greece). Geologisches Jahrbuch 23, 97–164.

Ambraseys, N.N., 1970. Some characteristic features of the North Anatolian Fault Zone. Tectonophysics 9, 143–165.

Ambraseys, N., Zatopek, A., 1968. The Varto Ustukran earthquake of 19 August 1966. Bulletin of the Seismological Society of America 58, 47–102.

Andrieux, J., Over, S., Poisson, A., Bellier, O., 1995. The North Anatolian Fault Zone: distributed Neogene deformation in its northward convex part. Tectonophysics 243, 135–154.

Angelier, J., 1990. Inversion of field data in fault tectonics to obtain the original stress. A new rapid direct inversion method by analytical means. Geophysical Journal International 1003, 363–376.

Arger, J., Mitchell, J., Westaway, R., 1996. In: Neogene and Quaternary Volcanism of Eastern Turkey: Potassium–Argon Dating and its Tectonic Implications, Open-file Science Reports, 1. Technosciences, Newcastle upon Tyne.

Arpat, E., Şaroğlu, F., 1975. Türkiye'deki bazi önemli genç tektonik olaylar. (On some important young tectonic events in Turkey.) Türkiye Jeoloji Kurumu Bülteni 18, 91–110.

Barka, A.A., 1985. Geology and tectonic evolution of some Neogene–Quaternary basins in the North Anatolian Fault zone. In: Ketin Symposium. Geological Society of Turkey, Special Publication, pp. 209–227.

Barka, A.A., 1992. The North Anatolian Fault Zone. Annales Tectonicae 6, 164–195.

Barka, A.A., 1996. Slip distribution along the North Anatolian fault associated with the large earthquakes of the period 1939–1967. Bulletin of the Seismological Society of America 86, 1238–1254.

Barka, A.A., Gülen, L., 1988. New constrain on age and total displacements of the North Anatolian Fault zone: implications for tectonics of the Eastern Mediterranean region. In: Koçyiğit, A., Altiner, D. (Eds.), 1987 Melih Tokay Geology Symposium. Middle East Technical University Special Publication, Ankara, Turkey.

Barka, A.A., Hancock, P.L., Robertson, A.M.F., 1984. Neotectonic deformation patterns in the convex-northwards arc of the North Anatolian Fault zone. In: Dixon, J.F. (Ed.), The Geological Evolution of the Eastern Mediterranean. Geological Society of London Special Publication 17, 763–774.

Barka, A.A., Kadinsky-Cade, K., 1988. Strike-slip fault geometry in Turkey and its influence on earthquake activity. Tectonics 7, 663–684.

Barka, A.A., Gülen, L., 1989. Complex evolution of the Erzincan basin (eastern Turkey). Journal of Structural Geology 11, 275–283.

Barka, A.A., Toksöz, M.N., Kadinsky-Cade, K., Gülen, L., 1987. The segmentation, seismicity and earthquake potential of the eastern part of the North Anatolian fault zone. In: International Report of the Earth Resources Laboratory. Massachusetts Institute of Technology.

Bellier, O., Över, S., Poisson, A., Andrieux, J., 1997. Recent temporal change in the stress state and modern stress field along the North Anatolian Fault Zone (Turkey). Geophysical Journal International 131, 61–86.

Bergougnan, H., 1987. Etudes géologiques dans l'est anatolien. Thesis, Paris 6 University, 86, 33.

Bozkurt, E., Koçyiğit, A., 1996. The Kazova basin: an active negative flower structure on the Almus Fault zone, a splay fault system on the North Anatolian Fault Zone, Turkey. Tectonophysics 265, 239–254.

Burke, K., Şengör, A.M.C., 1986. Tectonic escape in the evolution of the continental crust. In: Barazangi, M. (Ed.), Reflection Seismology, Continental Crust, Geodynamic Series, 14. American Geophysical Union Special Publication, pp. 41–51.

Chorowicz, J., Koffi, B., Chalah, C., Chotin, P., Collet, B., Poli, J.-T., Rudant, J.-P., Sykioti, O., Vargas, G., 1995a. Possibilités et limites de l'interprétation géologique des images (SAR) ERS-1. Bulletin de la Société Française de Photogrammétrie et Télédétection 138, 82–95.

Chorowicz, J., Luxey, P., Lyberis, N., Carvalho, J., Parrot, J.-F., Yürür, T., Gündoğdu, N., 1994. The Maras Triple Junction (Southern Turkey) based on digital Elevation Model and satellite imagery interpretation. Journal of Geophysical Research 99, 20225–20242.

Chorowicz, J., Luxey, P., Yürür, T., Rudant, J.-P., Gündoğdu, N., Lyberis, N., 1995b. Slip-motion estimation along the Ovacık fault near Ercinzan (Turkey) using ERS-1 radar image: Evidence of important deformation inside the Turkish plate. Remote Sensing of Environment 52, 66–70.

Dewey, J.F., 1976. Seismicity of Northern Anatolia. Bulletin of the Seismological Society of America 66, 843–868.

Dewey, J.F., 1988. Extensional collapse of orogens. Tectonics 7, 1123–1139.

Dewey, J.F., Şengör, A.M.C., 1979. Aegean and surrounding regions: complex multiplate and continuum tectonics in a convergent zone. Geological Society of America Bulletin 90, 84–92.

Dewey, J.F., Hempton, M.R., Kidd, W.S.F., Şaroğlu, F., Şengör, A.M.C., 1986. Shortening of continental lithosphere; the neotectonics of Eastern Anatolia, a young collision zone. In: Coward, M.P., Ries, A.C. (Eds.), Collision Tectonics. Geological Society of London Special Publication 19, 3–36.

Dhont, D., Chorowicz, J., Yürür, T., Köse, O., 1997. Polyphased displacement along the North Anatolian Fault Zone (Turkey). A model of 'pull-apart in pull-apart' basin. Terra Nova 9 (23–27 March), 390, European Union of Geosciences abstracts.

Dhont, D., Chorowicz, J., Yürür, T., Köse, O., 1998a. Polyphased block tectonics along the North Anatolian Fault in the Tosya basin area (Turkey). Tectonophysics 299, 213–277.

Dhont, D., Chorowicz, J., Yürür, T., Froger, J.-L., Köse, O., Gündoğdu, N., 1998b. Emplacement of volcanic vents and geodynamics of Central Anatolia, Turkey. Journal of Volcanology and Geothermal Research 85, 33–54.

Dungan, M.A., Lindstrom, M.M., McMillan, N.J., Moorbath, S., Hoefs, J., Haskin, L.A., 1986. Open system magmatic evolution of the Taos Plateau volcanic field, northern New Mexico, 1: The petrology and geochemistry of the Servitella basalt. Journal of Geophysical Research 91, 599–1371.

Fitton, J.G., James, D., Leeman, W.P., 1991. Basic magmatism associated with Late Cenozoic extension in the Western United State: Compositional variations in space and time. Journal of Geophysical Research 96, 13693–13711.

Gautier, P., Ballèvre, M., Brun, J.-P., Jolivet, L., 1990. Extension ductile et bassin mio-pliocène dans les cyclades (îles de Naxos et de Paros). Comptes Rendus de l'Académie des Sciences de Paris, Série II 310, 147–153.

Güleç, N., 1991. Crust-mantle interaction in Western Turkey: Implications from Sr and Nd isotope geochemistry of Tertiary and Quaternary volcanics. Geological Magazine 128, 417–435.

Gündoğdu, M.N., Vidal, P., Liewig, N., Cantagrel, J.-M., Froger, J.-L., 1994. Geochemical characteristics of Miocene–Quaternary volcanism along the North Anatolian Fault (NAF) zone, Turkey. Abstracts of the International Volcanological Congress, Ankara.

Hancock, P.L., Barka, A.A., 1981. Opposed shear senses inferred from neotectonic mesofracture systems in the North Anatolian Fault Zone. Journal of Structural Geology 5, 217–220.

Hempton, M.R., 1982. The North Anatolian fault and complexities of continental escape. Journal of Structural Geology 4, 502–504.

Hempton, M.R., 1987. Constraints on the Arabian plate motions; an extensional history of the Red Sea. Tectonics 6, 688–705.

Hempton, M.R., Dunne, L.A., 1984. Sedimentation in pull-apart basins: active examples in eastern Turkey. Journal of Geology 92, 513–530.

Irrlitz, W., 1971. Neogene and older Pleistocene of the intermontane basins in the Pontic region of Anatolia. Newsletters on stratigraphy 1, 33–36.

Jackson, J., 1994. Active tectonics of the Aegean region. Annual Review of Earth and Planetary Sciences 22, 239–271.

Jackson, J.A., McKenzie, D.P., 1984. Active tectonics of the Alpine–Himalayan belt between western Turkey and Pakistan. Geophysical Journal of the Royal Astronomical Society 77, 185–264.

Jackson, J.A., McKenzie, D.P., 1988. The relationship between plate motions and seismic moment tensors, and the rates of active deformation in the Mediterranean and Middle East. Geophysical Journal 93, 45–73.

Keller, J., Jung, D., Eckhardt, F.-J., Kreuzer, H., 1992. Radiometric ages and chemical characterization of the Galatean andesite massif, Pontus, Turkey. Acta Vulcanologica 2, 267–276.

Koçyiğit, A., 1989. Suehri basin: an active fault wedge basin on the North Anatolian fault zone, Turkey. Tectonophysics 137, 177–199.

Le Pichon, X., Angelier, J., 1979. The Hellenic arc and trench system: a key to the neotectonic evolution of the Eastern Mediterranean area. Tectonophysics 60, 1–42.

Le Pichon, X., Chamot-Rooke, N., Lallemant, S., Noomen, R., Veis, G., 1995. Geodetic determination of the kinematics of central Greece with respect to Europe: Implications for eastern Mediterranean tectonics. Journal of Geophysical Research 100, 12675–12690.

Lyberis, N., Yürür, T., Chorowicz, J., Kasapoğlu, E., 1992. The East Anatolian Fault: an oblique collisional belt. Tectonophysics 204, 1–15.

Mann, P., Hempton, M.R., Dwight, C.B., Burke, K., 1983. Development of pull-apart basins. Journal of Geology 91, 529–554.

McKenzie, D., 1972. Active tectonics of the Mediterranean region. Geophysical Journal of the Royal Astronomical Society 30, 109–185.

McKenzie, D., 1978. Active tectonics of the Alpine–Himalayan belt: the Aegean Sea and surrounding regions. Geophysical Journal of the Royal Astronomical Society 55, 217–254.

McKenzie, D., Jackson, J., 1983. The relationship between strain rates, crustal thickening, palaeomagnetism, finite strain and fault movements within a deforming zone. Earth and Planetary Sciences Letters 65, 182–202.

Mercier, J.-L., Sorel, D., Vergely, P., 1989. Extensional tectonic regimes in the Aegean basins during the Cenozoic. Basin Research 2, 49–71.

Okay, A.I., 1989. Tectonic units and sutures in the Pontides, Northern Turkey. In: Şengör, A.M.C. (Ed.), Tectonic Evolution of the Tethyan Region, NATO ASI Series, Series C 259 , , pp. 109–116.

Oral, M.B., Robert, E.R., Toksöz, N.M., Barka, A.A., Kinik, I., 1993. Preliminary results of 1988 and 1990 GPS measurements in western Turkey and their tectonic implications. Crustal Geodynamics 23, 407–416.

Pasquarè, G., Poli, S., Vezzoli, L., Zanchi, A., 1988. Continental arc volcanism and tectonic setting in Central Anatolia, Turkey. Tectonophysics 146, 217–230.

Pearce, J.A., Bender, J.F., De Long, S.E., Kidd, W.S.F., Low, P.J., Güner, Y., Şaroğlu, F., Yılmaz, Y., Moorbath, S., Mitchell, G., 1990. Genesis of collision volcanism in Eastern Anatolia, Turkey. Journal of Volcanology and Geothermal Research 44, 189–229.

Philip, H., Cisternas, A., Gvishiani, A., Gorshkov, A., 1989. The Caucasus: an actual example of the initial stages of continental collision. Tectonophysics 161, 1–21.

Poisson, A., Temiz, H., Gürsoy, H., 1992. Pliocene thrust tectonics in the Sivas Basin near Hafik (Turkey): Southward fore thrusts and associate northward back thrusts. Bulletin of the Faculty of Engineering Cumhuriyet University 9, 18–26.

Reilinger, R.E., McClusky, S.C., Oral, M.B., King, R.W., Toksoz, M.N., Barka, A.A., Kinik, I., Lenk, O., Sanli, I., 1997. Global Positioning System measurements of present-day crustal movements in the Arabia–Africa–Eurasia plate collision zone. Journal of Geophysical Research 102, 9983–9999.

Şaroğlu, F., 1988. Age and offset of the North Anatolian fault. Middle East Technical University Journal of Pure and Applied Science 21, 65–79.

Şaroğlu, F., Yılmaz, Y., 1989. Example of triple junction of intersecting faults in Turkey: Karlıova region. Abstract of the 28th International Geological Congress 3, 3–24.

Şaroğlu, F., Yılmaz, Y., 1991. Geology of the Karlıova region: intersection of the North Anatolian and East Anatolian transform faults. Bulletin of the Technical University of Istanbul 44, 475–493.

Şengör, A.M.C., 1979. The North Anatolian transform fault: its age, offset and tectonic significance. Journal of the Geological Society of London 136, 269–282.

Şengör, A.M.C., Barka, A.A., 1992. Evolution of the escape-related strike-slip systems, implications for distributions of collisional orogens. In: 29th International Congress Abstracts, Kyoto, Japan, pp. 1–232.

Şengör, A.M.C., Burke, K., Dewey, J.F., 1982. Tectonics of the North Anatolian Transform Fault. In: Iskara, M., Vogel, A., Friedr, A. (Eds.), Multidisciplinary Approach to Earthquake Prediction. Vieweg and Sohn, Braunschweig–Wiesbaden, pp. 3–22.

Şengör, A.M.C., Görür, N., Şaroğlu, F., 1985. Strike-slip faulting and related basin formation in zones of tectonic escape: Turkey as a case study. In: Biddle, K.T., Christie-Blick, N. (Eds.), Strike-Slip Deformation, Basin Formation and Sedimentation. Society of Economy, Palaeontology and Mineralogy Special Publication 37, 227–264.

Seyitoğlu, G., Scott, B., 1992. Late Cenozoic volcanic evolution of the Northeastern Aegean region. Journal of Volcanology and Geothermal Research 54, 157–176.

Stein, R.S., Barka, A.A., Dieterich, J.H., 1997. Progressive failure on the North Anatolian fault since 1939 by earthquake stress triggering. Geophysical Journal International 128, 594–604.

Suzanne, P., Lyberis, N., 1992. Mécanisme de déformation le long de la partie orientale de la Faille Nord Anatolienne. Annales Tectonicae 6, 26–40.

Suzanne, P., Lyberis, N., Chorowicz, J., Nurlu, M., Yürür, T., Kasapoğlu, E., 1990. La géométrie de la Faille Nord Anatolienne à partir d'images Landsat-MSS. Bulletin de la Société Géologique de France 8, 589–599.

Tatar, Y., 1975. Tectonic structures along on the North Anatolian fault zone northeast of Refahiye (Erzincan). Tectonophysics 25, 401–409.

Tatar, Y., 1978. Tectonic investigations on the North Anatolian fault zone between Erzincan and Refahiye. Publication of the Institute of Earth Sciences of Hacettepe University 4, 136–201.

Tatar, O., Piper, J.D.A., Park, R.G., Gürsoy, H., 1995. Paleomagnetic study of block rotations in the Niksar overlap region of the North Anatolian Fault zone, central Turkey. Tectonophysics 244, 251–266.

Tchalenko, J.S., 1977. A reconnaissance of the seismicity and tectonics at the northern border of the Arabian plate (Lake Van region). Revue de Géographie Physique et de Géologie Dynamique 19, 189–208.

Temel, A., 1992. Kapadokya eksplosif volkanizmasinin petrolojik ve jeokimyasal özellikleri. Thesis, Hacettepe University, pp. 208.

Toprak, V., Göncüoğlu, M.C., 1993. Tectonic control on the development of the Neogene–Quaternary Central Anatolian volcanic province, Turkey. Geological Journal 28, 357–369.

Trifonov, V.G., Karakhanian, A.S., Kozhurin, A.I., 1994. Major active faults of the collision area between the Arabian and the Eurasian plates. In: Bolt, B.A., Amirbekian, R. (Eds.), Continental Collision Zone Earthquakes and Seismic Hazard Reduction. Proceedings of the International Conference at Yerevan–Sevan, Armenia, 1–6 October 1993. IASPEI, pp. 56–76.

Tutkun, S.-Z., Hancock, P.-L., 1990. Tectonic landform expressing strain at the Karlıova triple junction (E. Turkey). Annales Tectonicae 4, 182–195.

Wallace, R.E., 1968. Earthquake of the August 19, 1968, Varto area, eastern Turkey. Bulletin of the Seismological Society of America 58, 11–45.

Westaway, R., 1994. Present-day kinematics of the Middle East and eastern Mediterranean. Journal of Geophysical Research 99, 15437–15464.

Westaway, R., Arger, J., 1996. The Gölbasi basin, southern Turkey: a complex discontinuity in a major strike-slip fault zone. Journal of the Geological Society of London 153, 729–744.

Yılmaz, Y., 1990. Comparison of young volcanic associations of western and Eastern Anatolia formed under a compressional regime: a review. Journal of Volcanology and Geothermal Research 44, 69–87.

Yılmaz, Y., 1993. New evidence and model of the evolution of the southeast Anatolian orogen. Geological Society of America Bulletin 105, 252–271.

Yürür, M.T., Chorowicz, J., 1998. Recent volcanism, tectonics and plate kinematics near the junction of the African, Arabian and Anatolian plates in the Eastern Mediterranean. Journal of Volcanology and Geothermal Research 85, 1–15.

Yürür, M.T., Köse, O., Buket, E., Demirbas, H., Güven, A.R., 1998. Recent tectonics and volcanism in the eastern vicinity of Karlıova junction zone, eastern Turkey. Abstracts of the Third International Turkish Geology Symposium, Ankara, 96.